*The Canadian Mineralogist*
Vol. 45, pp. 607-629 (2007)
DOI: 10.2113/gscanmin.45.3.607

# PROTOLITH COMPOSITION OF CORDIERITE–GEDRITE BASEMENT ROCKS AND GARNET AMPHIBOLITE OF THE BEARPAW LAKE AREA OF THE THOR–ODIN DOME, MONASHEE COMPLEX, BRITISH COLUMBIA, CANADA

Alana M. HINCHEY[§] and Sharon D. CARR[¶]

*Ottawa–Carleton Geoscience Center, Department of Earth Sciences, Carleton University, Ottawa, Ontario K1S 5B6, Canada*

## Abstract

The Thor–Odin dome of the Monashee complex, southeastern Canadian Cordillera, British Columbia, contains basement gneiss of North American tectonic affinity, including a distinctive cordierite–gedrite rock that is restricted in occurrence to the basement rocks and a regionally occurring garnet amphibolite. All of these rocks were penetratively deformed and metamorphosed at upper-amphibolite to lower-granulite facies conditions in the Cordilleran orogeny during the Late Cretaceous to Paleocene. The cordierite–orthoamphibole (dominantly gedrite) unit appears to define a discontinuous marker horizon or horizons within the Paleoproterozoic basement paragneiss. The cordierite–gedrite rocks have a unique bulk-rock composition that is characterized by depletions in the alkali elements and Ca, and enrichments in Al, Mg and Fe. They have flat rare-earth element (REE) patterns, depletions in most low field-strength elements (LFSE), and enrichments in high field-strength elements (HFSE). The measured $^{87}Sr/^{86}Sr$ values for these rocks vary from 0.74923 to 0.85962, and the $\varepsilon Nd_{(today)}$ values vary from –15.3 to –20.6. The cordierite–gedrite rocks are interpreted as Paleoproterozoic mafic volcanic rocks that were hydrothermally altered, likely prior to metamorphism. Hydrothermal alteration explains their distinctive bulk-rock composition. Interlayered and spatially associated lenses of garnet amphibolite are of uncertain age, although they are likely Precambrian, on the basis of their Nd isotopic composition. The garnet amphibolite rocks are characterized by high Mg and Ti values and depletions in the alkali elements. They have flat REE patterns, depletions in most LFSE and enrichments in HFSE. The garnet amphibolite samples have measured $^{87}Sr/^{86}Sr$ values that vary from 0.70953 to 0.74319, and $\varepsilon Nd_{(today)}$ values that vary from –0.8 to –7.3. The garnet amphibolite rocks are interpreted as Proterozoic metamorphosed mafic dykes or possibly volcanic rocks that postdated the formation of the protolith of the cordierite–gedrite rocks.

*Keywords*: Thor–Odin dome, Monashee complex, cordierite–gedrite rocks, garnet amphibolite, chemical composition, Nd isotopes, Sr isotopes, basement rocks, British Columbia.

## Sommaire

Le dôme de Thor–Odin, faisant partie du complexe de Monashee, dans le sud–est des Cordillères canadiennes, en Colombie-Britannique, contient un socle gneissique d'affinité tectonique nord-américaine, y inclus une unité distinctive à cordiérite–gédrite qui est restreinte aux roches du socle et associée à une amphibolite grenatifère distribuée régionalement. Toutes ces roches ont été fortement déformées au faciès amphibolite supérieur et granulite inférieur au cours de l'orogenèse de la Cordillère, allant du Crétacé tardif au Paléocène. L'unité à cordiérite–orthoamphibole (la gédrite, surtout) semble définir un marqueur discontinu en un ou plusieurs horizons au sein du socle paragneissique paléoproterozoïque. Les roches à cordiérite–gédrite possèdent une composition globale dépourvue en alcalins et en Ca, et enrichie en Al, Mg et Fe. Les tracés des terres rares sont plats; il y a appauvrissement dans la plupart des éléments à faible champ électrostatique, et enrichissement en éléments à champ électrostatique élevé. Les valeurs mesurées de $^{87}Sr/^{86}Sr$ varient de 0.74923 à 0.85962, et les valeurs de $\varepsilon Nd_{(aujourd'hui)}$ varient de –15.3 à –20.6. A notre avis, ces roches paléoprotérozoïques seraient d'origine volcanique mafique; elles auraient subi une altération hydrothermale, probablement avant leur métamorphisme, ce qui rendrait compte de leur composition globale distinctive. Les lentilles intercalées d'amphibolite grenatifère ont un âge incertain, mais probablement précambrien, vue la composition isotopique du Nd. Les amphibolites grenatifères possèdent des valeurs élevées de Mg et de Ti, et un appauvrissement en alcalins. Elles font preuve d'un profil des terres rares horizontal, un appauvrissement en éléments à faible champ électrostatique, et un enrichissement en éléments à champ électrostatique élevé. Elles montrent des valeurs de $^{87}Sr/^{86}Sr$ entre 0.70953 et 0.74319, et des valeurs de $\varepsilon Nd_{(aujourd'hui)}$ entre –0.8 et –7.3. Les amphibolites grenatifères seraient des filons mafiques protérozoïques métamorphisés, ou bien des roches volcaniques mises en place après la formation du protolithe des roches à cordiérite–gédrite.

(Traduit par la Rédaction)

*Mots-clés*: dôme de Thor–Odin, complexe de Monashee, roches à cordiérite–gédrite, amphibolite grenatifère, composition chimique, isotopes de Nd, isotopes de Sr, roches du socle, Colombie-Britannique.

§ *Present address*: Geological Survey, Department of Natural Resources, Government of Newfoundland and Labrador, P.O. Box 8700, St. John's, Newfoundland A1B 4J6, Canada. *E-mail address*: alanahinchey@gov.nl.ca
¶ *E-mail address*: scarr@ccs.carleton.ca

## Introduction

Cordierite–orthoamphibole rocks occur as lenses and boudinaged layers in Paleoproterozoic basement paragneiss of the Thor–Odin dome, in the Monashee complex of southeastern British Columbia. The origin of the cordierite–orthoamphibole (gedrite–anthophyllite) rocks is enigmatic, as their composition is not easily explained as being either of sedimentary or igneous origin. These rocks are marked by enrichments in Mg, Al, and Fe, and depletions in the alkali elements, and Ca. They are of interest because the Precambrian history of the Thor–Odin area is poorly constrained owing to a strong overprint of pervasive high-grade metamorphism, deformation, and anatexis associated with reworking of the crust in the Cretaceous–Tertiary during construction of the Cordilleran orogeny, and subsequent exhumation of the Monashee complex.

Genetic models for the evolution of cordierite–orthoamphibole rocks are diverse, but generally fall into two groups, based on whether or not the protoliths were affected by chemical alteration (metasomatism) before or during metamorphism. The first model involves synmetamorphic metasomatism, in which Fe and Mg may be introduced by diffusion or infiltration of hydrothermal fluid into a range of rock types (*i.e*., Eskola 1914, Irving & Ashley 1976). A second model invokes partial melting, likely of a pelitic sediment or a metavolcanic protolith, whereby cordierite–orthoamphibole rocks represent the residuum after extraction of granitic melt (*i.e*., Grant 1968, Hoffer & Grant 1980). In a third model, the cordierite–orthoamphibole rocks form *via* metamorphism of a weathered horizon, *i.e*. these rocks are a paleoregolith or paleosol (*i.e*., Gable & Sims 1969, Young 1973). In a fourth model, the cordierite–orthoamphibole rocks represent volcanic rocks that were hydrothermally altered prior to metamorphism (*i.e*., Vallance 1967, Robinson & Jaffe 1969a, b, James *et al*. 1978, Schumacher 1988, Smith *et al*. 1992, Peck & Smith 2005). This is the most commonly invoked model and usually involves seawater as the hydrothermal fluid (Spear 1993).

In this paper, the origin and geological significance of the cordierite–gedrite rocks in the Thor–Odin dome are addressed. This unit may define a dismembered pseudostratigraphy within the basement paragneiss, and outcrop on the limbs of folds, as suggested by Duncan (1984). Major and trace-element geochemical studies, in combination with Rb–Sr and Sm–Nd isotopic studies, were carried out to address the question of petrogenesis of cordierite–gedrite rocks, as well as nearby garnet amphibolite. Further understanding of their modes of formation has implications for the tectonic evolution of the Thor–Odin dome.

## Geological Setting

The Monashee complex in southeastern British Columbia contains exposures of Paleoproterozoic basement rocks that are part of the deepest exposed structural levels in the southern Canadian Cordillera (Fig. 1). The Thor–Odin dome of the southern Monashee complex is a structural culmination of Paleoproterozoic basement rocks infolded with younger Paleoproterozoic to Paleozoic (?) supracrustal or cover rocks (Reesor & Moore 1971, Parkinson 1992; Fig. 2). Both the basement and the cover sequence experienced polydeformation (Williams & Jiang 2005), high-grade metamorphism (Norlander *et al*. 2002) and Early Tertiary anatexis (Vanderhaeghe *et al*. 1999, Hinchey *et al*. 2006). Pervasive Cretaceous (?) to Eocene Cordilleran deformation transposed and overprinted Precambrian relationships and structures (Williams & Jiang 2005).

The panel of rocks that structurally overlies and in map view surrounds the Thor–Odin dome on the southern and western sides is termed the Middle Crustal Zone after Carr (1991) [*cf*. the Selkirk Allochthon of Brown *et al*. (1986) and the Middle Unit of Vanderhaeghe *et al*. (1999) and Norlander *et al*. (2002)]. The nature and significance of deformation within the high-grade rocks, and the relationship between the Middle Crustal zone and the Thor–Odin dome, are currently debated, and a number of authors have proposed contrary tectonic models (Brown 2004, Teyssier *et al*. 2005, Williams & Jiang 2005, Glombick 2005, Carr & Simony 2006, Brown & Gibson 2006). At the latitude of the Thor–Odin dome, high-grade rocks of both the dome and the Middle Crustal Zone are bounded on the eastern and western margins by generally north-striking, outward-dipping Eocene normal faults (Fig. 1; Parrish *et al*. 1988, Teyssier *et al*. 2005, and references therein). The eastern margin is bounded by the largely 58–48 Ma Columbia River fault (CR), and the western margin, by the 56–45 Ma Okanagan Valley – Eagle River fault system (OV–ER; Parrish *et al*. 1988, Johnson 2006, and references therein).

Within the Monashee complex, Early Tertiary ductile involvement of the basement has been identified in both the northern Frenchman Cap dome and the southern Thor–Odin dome (Crowley 1999, Vanderhaeghe *et al*. 1999, Crowley *et al*. 2001, Hinchey 2005), although the style of basement involvement is apparently different in the two domes. In the Frenchman Cap dome, rocks in the upper structural levels of the basement-cored dome experienced high-grade metamorphism from *ca*. 80 to 50 Ma (Parrish 1995, Crowley & Parrish 1999, Gibson *et al*. 1999); however, a boundary delimiting the base of Eocene Cordilleran deformation has been located at deep structural levels, below which

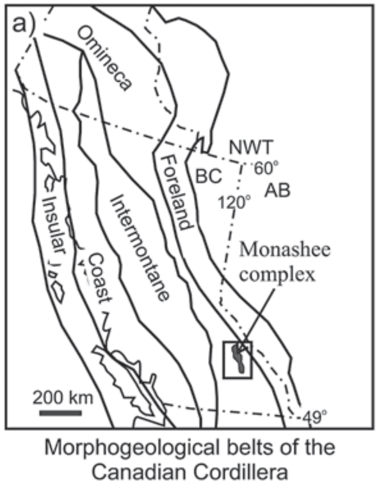


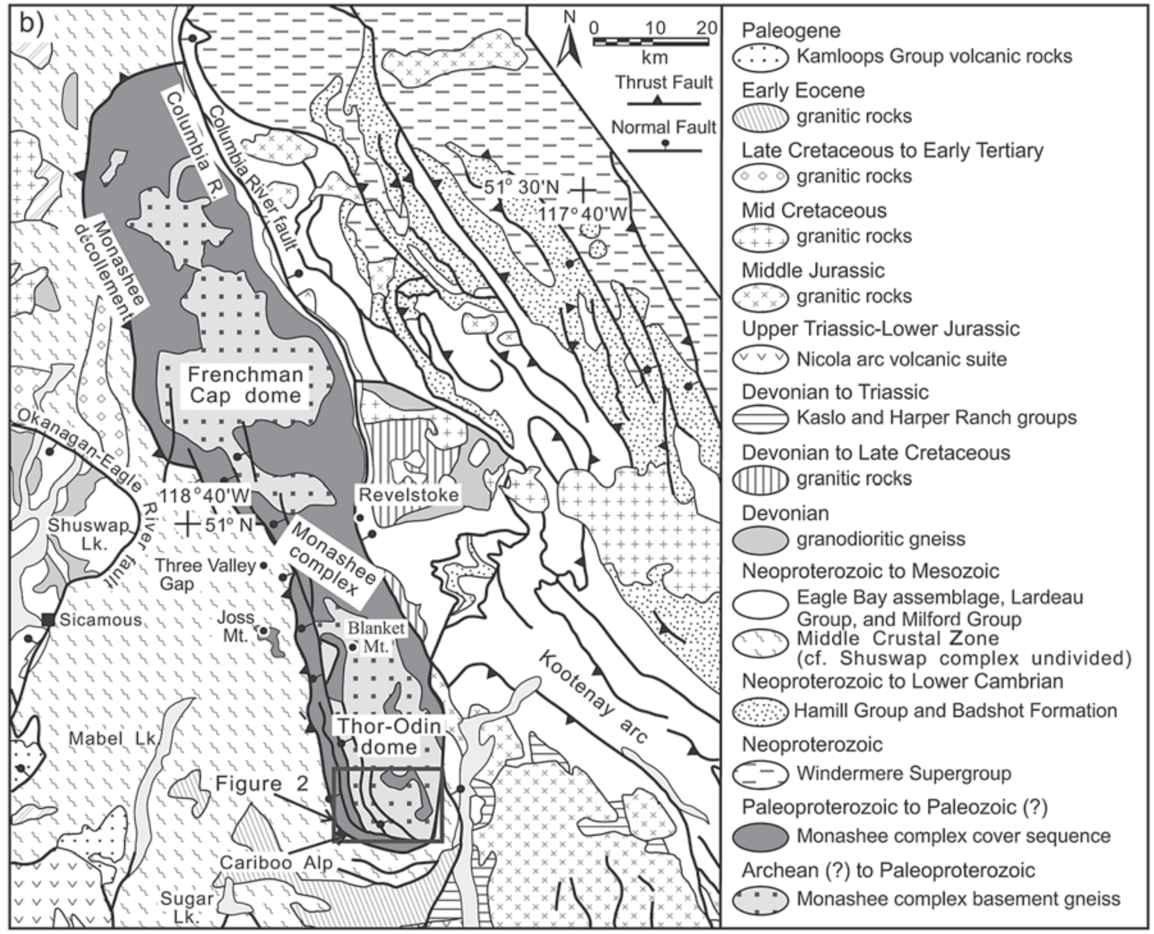


FIG. 1. (a) The five morphogeological belts of the Cordillera (Wheeler & McFeely 1991). (b) Tectonic assemblage map of southeastern Omineca belt, British Columbia (modified after Wheeler & McFeely 1991), outlining the lithological units of the Monashee complex and surrounding area. The box in the Thor–Odin dome area delineates Figure 2.

Precambrian relationships greater than 1.8 Ga in age are preserved (Crowley 1999, Crowley *et al.* 2001). In contrast, studies of the Thor–Odin dome confirm that all structural levels experienced penetrative high-grade metamorphism and anatexis during the Paleocene to Eocene (Vanderhaeghe *et al.* 1999, Norlander *et al.* 2002, Hinchey 2005, Hinchey *et al.* 2006). In the Thor–Odin dome, products of Precambrian metamorphism and deformation have been pervasively overprinted by Cordilleran deformation and metamorphism. This is in contrast to the Frenchman Cap dome, where Precambrian metamorphism and deformation are preserved at deep structural levels, including 2.06 Ma monazite ages, 1.85 Ga titanite ages, and a gneissosity that apparently predates 1.85 Ga (Parrish 1995, Crowley 1999). A focus of this paper is the elucidation of part of the Precambrian history by understanding the formation of the cordierite–gedrite basement rocks in the Thor–Odin dome. The rocks studied are exposed in the Bearpaw Lake area (Figs. 2, 3), in the southwestern portion of the dome.

## The Bearpaw Lake Area

### *Geology*

The Bearpaw Lake area (Fig. 3) is characterized by Paleoproterozoic basement rocks dominated by a) hornblende–biotite granodiorite migmatitic orthogneiss, and b) compositionally heterogeneous garnet–sillimanite quartzofeldspathic migmatitic paragneiss. The garnet–sillimanite quartzofeldspathic paragneiss is interlayered at the scale of tens of meters with muscovite–biotite quartzofeldspathic diatexite paragneiss and hornblende–biotite quartzofeldspathic paragneiss. The package of rocks also contains boudinaged layers of cordierite–gedrite rocks, dykes of garnet amphibolite, and infolded quartzite and calc-silicate. The gneiss package trends southeast and dips ~70° to the southwest. The lenses of cordierite–gedrite rock and garnet amphibolite were likely boudinaged during deformation associated with $F_2$ folding, which was ongoing at *ca.* 56 Ma on the basis of zircon from folded veins of leucosome (Fig. 3; Hinchey *et al.* 2006).

Protolith ages are constrained by U–Pb geochronology studies of zircon from basement orthogneiss, which yield upper intercept dates of 1960 ± 45, 1934 ± 6 and 1874 ± 21 Ma, and are interpreted as crystallization ages (Wanless & Reesor 1975, Parkinson 1992). Deposition of part of the basement paragneiss occurred between *ca.* 2.2 Ga and 1.9 Ga, on the basis of a study of detrital zircon in a basement paragneiss that was apparently intruded by *ca.* 1.9 Ga plutons (Parkinson 1992). Other layers within the basement paragneiss may be younger than *ca.* 1.8 Ga, on the basis of the 1.8 Ga date of the youngest concordant detrital grains from basement paragneiss (Vanderhaeghe *et al.* 1999, Kuiper 2003, Hinchey 2005, Hinchey *et al.* 2006).

Lenses of cordierite–gedrite rocks are 15 to 50 meters thick and up to 500 meters long (Fig. 3). They parallel the pervasive $S_2$ transposition foliation and strike at 135–142° to the southeast. Known occurrences of these rocks, in the southwestern portion of the dome, are shown in Figure 2. The cordierite–gedrite rocks are documented within the basement paragneiss only, where they occur on the limbs of $F_2$ isoclines. At least locally, they seem to define a discontinuous marker-horizon(s).

Garnet amphibolite occurs as discontinuous boudinaged lenses that range from 10 to 20 meters thick and up to 400 meters long (Fig. 3). The amphibolite lenses parallel the pervasive $S_2$ transposition foliation and strike at 133–150° to the southeast. In the study area, the lenses of garnet amphibolite are observed only within the basement paragneiss, are not observed crosscutting the cordierite–gedrite rocks, and are documented throughout the Thor–Odin dome (Reesor & Moore 1971, Parkinson 1992). However, elsewhere in the dome, concordant boudinaged amphibolites have been mapped within both the basement para- and orthogneiss and cover sequence (Parkinson 1992). Attempts have been made to correlate the amphibolite with regional mafic suites. Specifically, comparisons were made between Nd isotopic signatures of amphibolite from the Thor–Odin dome and: a) the mafic Moyie sills (1.5 Ga) of the Middle Proterozoic Belt–Purcell Supergroup (Burwash *et al.* 1988, Burwash & Wagner 1989), and b) the mafic volcanic rocks associated with the Horsethief Creek Group (~760 Ma; Devlin *et al.* 1988, Sevigny & Thériault 2003) of the Late Proterozoic Windermere Supergroup. However, owing to a wide range in isotopic values of the amphibolite samples and a limited dataset, correlation was not possible (Parkinson 1992).

For the purpose of evaluating their petrogenesis, the cordierite–gedrite samples are plotted on geochemical and isotopic diagrams with the garnet amphibolite samples. This is done for purposes of comparison; the amphibolite rocks occur regionally, they have been the subject of previous geochemical studies (Parkinson 1992, Sevigny 1988), and their composition more closely approximates that of a typical metamorphosed mafic rock than that of the cordierite–gedrite rock. For the purpose of evaluating the isotopic signatures, values are calculated at an age of ~760 Ma, which is the Nd $T_{DM}$ model age of the Horsethief Creek mafic volcanic suite (Devlin *et al.* 1988). This is interpreted as the likely lower age-constraint for the garnet amphibolite based on $T_{DM}$ model age, the timing of continental rifting of western North America, and correlations with regional amphibolites (Parkinson 1992, Ross 1991, Sevigny & Thériault 2003, this study). There are no direct U–Pb geochronological constraints on age on either cordierite–gedrite or amphibolite rocks in the Thor–Odin dome. An amphibolite boudin in the Middle Crustal Zone near Three Valley gap gives a U–Pb (zircon) upper intercept age of 1571 ± 76 Ma,

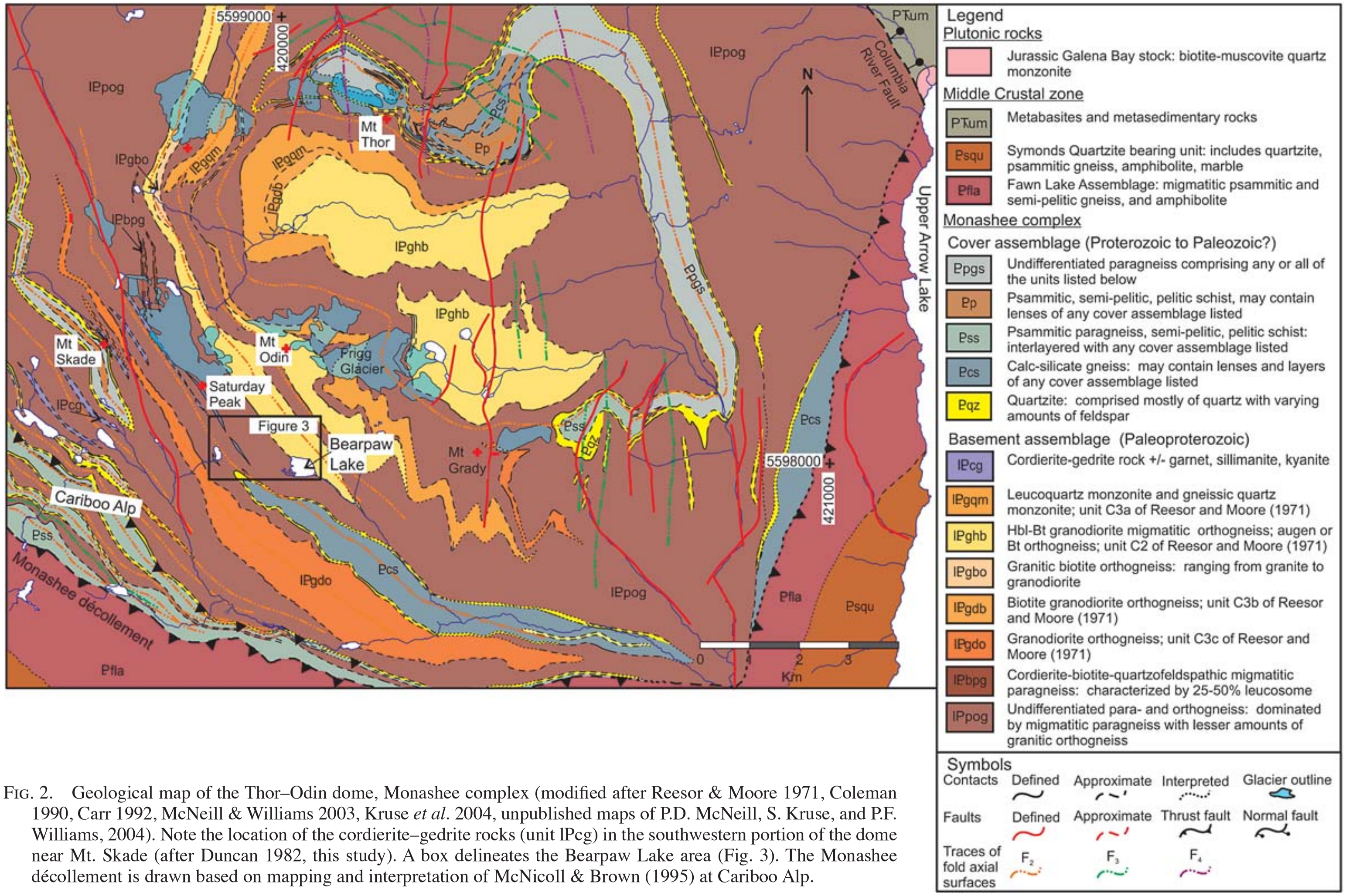


FIG. 2. Geological map of the Thor–Odin dome, Monashee complex (modified after Reesor & Moore 1971, Coleman 1990, Carr 1992, McNeill & Williams 2003, Kruse *et al*. 2004, unpublished maps of P.D. McNeill, S. Kruse, and P.F. Williams, 2004). Note the location of the cordierite–gedrite rocks (unit lPcg) in the southwestern portion of the dome near Mt. Skade (after Duncan 1982, this study). A box delineates the Bearpaw Lake area (Fig. 3). The Monashee décollement is drawn based on mapping and interpretation of McNicoll & Brown (1995) at Cariboo Alp.

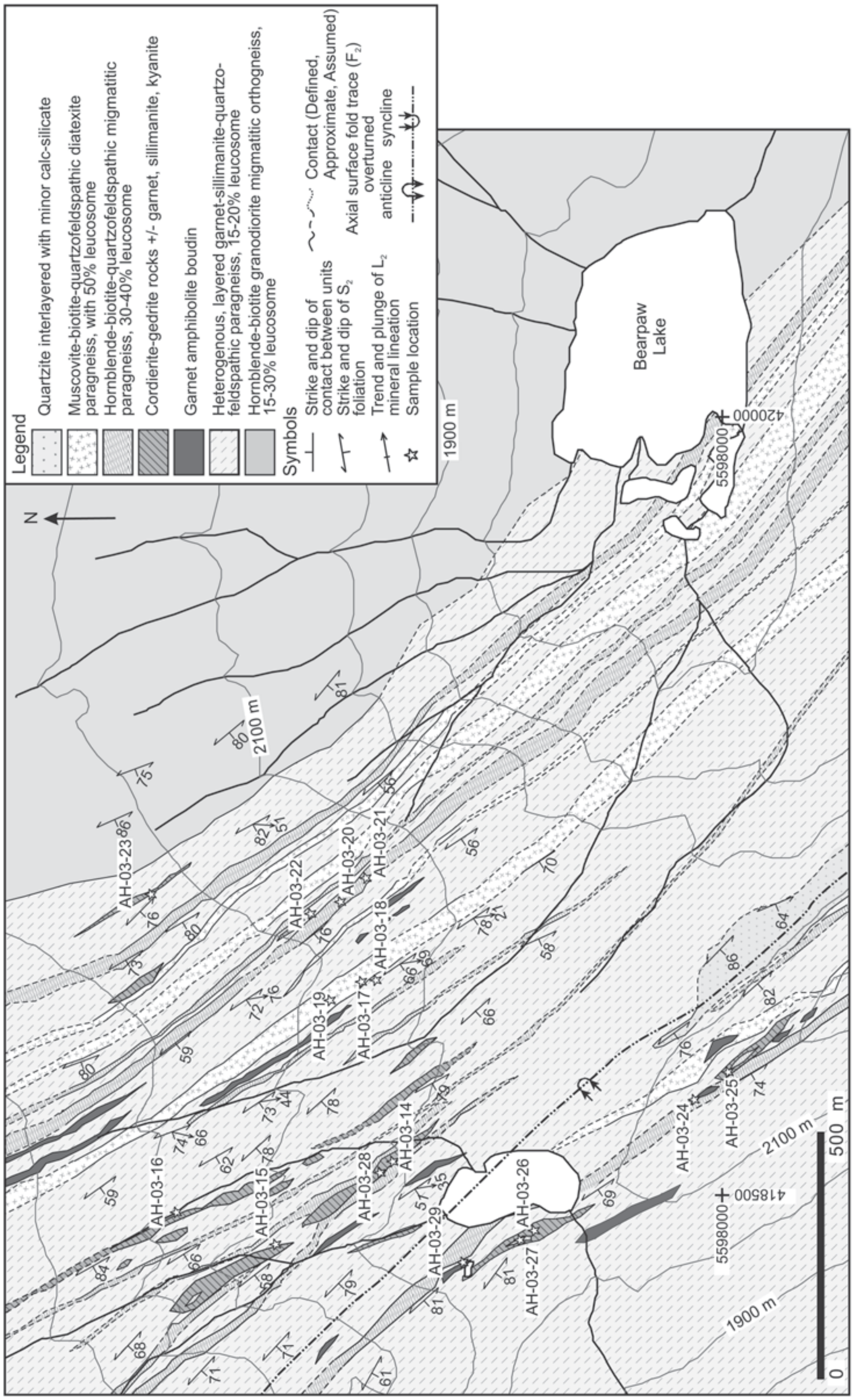


FIG. 3. Geological map of the Bearpaw Lake area, Thor–Odin dome, Monashee complex (mapping by A.M. Hinchey).

interpreted as the age of igneous crystallization, and a lower intercept age of 73.4 ± 1.7, Ma interpreted as the timing of metamorphism (Parkinson 1992). This amphibolite locality is ~5 km structurally higher than the Bearpaw Lake area; however, given the amount of Paleogene transposition, strain, and deformation (*i.e.*, km-scale isoclinal folds) in the intervening rocks (Hinchey *et al*. 2006), the relationship between the two localities of amphibolite is ambiguous.

Thermobarometry studies in the Bearpaw Lake area indicate that basement rocks underwent decompression from the kyanite zone (P > 8–10 kbar) to the sillimanite–cordierite zone (P < 5 kbar) at temperatures of *ca*. 750°C, up to a maximum of 800°C, based on the mineral assemblages and reaction textures (Norlander *et al*. 2002). On the basis of complex symplectitic textures preserved in basement cordierite–gedrite rocks and in garnet amphibolite boudins, Norlander *et al*. (2002) concluded that the peak episode of regional metamorphism occurred in the Tertiary, as these textures would not have survived a subsequent metamorphic event. This is consistent with U–Pb (zircon) geochronology studies indicating that metamorphism and penetrative deformation of the basement rocks of the Thor–Odin dome were ongoing during the Paleogene at *ca*. 56 to 50 Ma (Vanderhaeghe *et al*. 1999, Hinchey 2005, Teyssier *et al*. 2005, Hinchey *et al*. 2006; this study). Peak metamorphism culminated in the onset of melting and the production of leucosome (Vanderhaeghe *et al*. 1999, Norlander *et al*. 2002, Hinchey 2005, Hinchey *et al*. 2006).

### *Lithology and petrology*

The cordierite–gedrite rocks are very coarse grained and display complex symplectitic intergrowths. Gedrite crystals are up to 25 cm long, and garnet is up to 15 cm in diameter. In hand sample, the typical assemblage of minerals includes: biotite, sillimanite, kyanite, quartz, spinel, garnet and cordierite (Fig. 4a). Norlander *et al*. (2002) distinguished between gedrite rocks that contain garnet and those that are sapphirine-bearing; however, this distinction is not possible at the outcrop scale. All exposures of the cordierite–gedrite boudins contain garnet, at least locally, and thus the absence of garnet in thin section may reflect local small-scale breakdown reactions or compositional heterogeneity within the protolith. The contact between the cordierite–gedrite rocks and paragneiss generally contain mats of randomly oriented, coarse-grained sillimanite mantled by cordierite and corundum.

Gedrite, the most abundant mineral in the cordierite–gedrite rocks, occurs as prismatic crystals that define the $S_2$ foliation. Garnet occurs as porphyroblasts that contain abundant inclusions of cordierite, spinel, gedrite, and apatite (Fig. 4b). Cracks in the garnet grains are filled with grains of cordierite, gedrite, ilmenite, plagioclase and spinel. Kyanite has been partially to entirely replaced by a corundum + cordierite + ilmenite symplectite in the cores of the grains, and spinel + cordierite ± sapphirine in the rim area (Norlander *et al*. 2002). Cordierite occurs dominantly as an interstitial mineral between blades of gedrite. Sillimanite occurs as prismatic crystals or as a fibrous overgrowth on kyanite. Accessory biotite, quartz, apatite, spinel, ilmenite, and monazite are common. Further petrological descriptions related to determination of pressure–temperature conditions are described in Norlander *et al*. (2002). On the basis of mineralogy, the cordierite–gedrite rocks in the Thor–Odin dome were considered to be the product of hydrothermal alteration of mafic volcanic rocks, or a restite of partial melting (Duncan 1982, 1984).

The garnet amphibolite rocks are medium grained and hornblende-bearing, typically with garnet – hornblende – quartz – plagioclase ± clinopyroxene (Fig. 4c). Hornblende occurs both as interstitial grains in the matrix and as euhedral, tabular grains that define the $S_2$ foliation. Garnet porphyroblasts are 1–3 mm in diameter and contain few inclusions of plagioclase, biotite, ilmenite and rutile (Norlander *et al*. 2002). Grains of garnet are commonly rimmed by quartz + plagioclase symplectite (Fig. 4d). Accessory phases are ilmenite, biotite, apatite and monazite. Plagioclase and quartz are granoblastic, anhedral grains that dominate the matrix. Plagioclase commonly displays albite twinning, and quartz contains subgrains. Further petrological descriptions related to thermobarometry determinations for the garnet amphibolite rocks are described in Norlander *et al*. (2002).

## Analytical Data and Interpretation

### *Major and trace elements*

Compositions, expressed in terms of major-element oxides, recalculated to an anhydrous total of 100%, as well as concentrations of selected trace elements, were determined for all major map-units in the Bearpaw Lake area. Six samples of the cordierite–gedrite rock and four samples of garnet amphibolite were analyzed. The cordierite–gedrite samples are plotted with the garnet amphibolite for comparison (Fig. 5), as the amphibolite more closely approximates a typical metamorphosed mafic rock. Sample descriptions and locations are listed in Table 1. Representative compositions are presented in Table 2, and analytical methods are given in Appendix A. Four samples of quartzofeldspathic basement paragneiss and two samples of granodioritic basement orthogneiss from adjacent gneisses and from the core of the dome are plotted for comparison (data from Hinchey & Carr 2006).

The cordierite–gedrite samples show a large range in $SiO_2$ contents, from 28.1 to 53.1 wt.% (Table 2), with one of the samples (AH–03–25) having a notably low concentration of $SiO_2$, 28.1 wt.%, attributed to the large percentage of hercynite, making up approximately couleur pas nécessaire



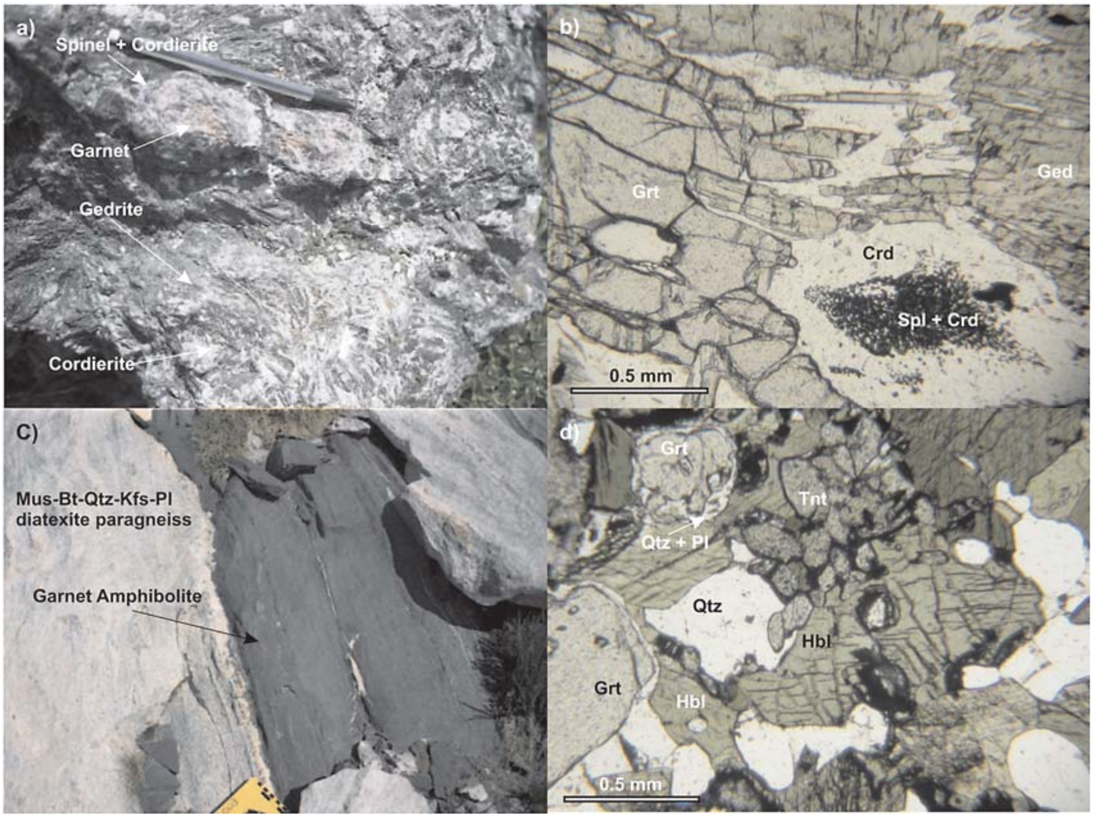


FIG. 4. Photo (a) shows a garnet porphyroblast with a reaction rim of cordierite–spinel surrounded by coarse-grained crystals of gedrite. Photo (b) shows garnet porphyroblasts, symplectite of spinel and cordierite, interstitial grains of cordierite and euhedral crystals of gedrite. Photo (c) shows a lens of garnet amphibolite hosted in the ms–bt quartzofeldspathic diatexite paragneiss. Photo (d) shows garnet porphyroblasts rimmed by quartz and plagioclase, euhedral grains of hornblende and titanite, and interstitial quartz grains.

25 wt.% of its bulk-rock composition. In all samples, $Al_2O_3$ ranges from 12.8 to 23.1 wt.%. Concentrations of CaO and $Na_2O$ are low, with values ranging from 6.0 to 0.2 wt.% and 0.2 to 0.9 wt.%, respectively. The samples have 12.4 to 18.1 wt.% MgO, 1.6 to 3.9 wt.% $Fe_2O_3$, 0.1 to 0.3 wt.% MnO, and 0.3 to 3.7 wt.% $TiO_2$ (Table 2). Compared to the cordierite–gedrite samples, the garnet amphibolite samples have a narrower range in $SiO_2$, from 45.9 to 51.0 wt.%, and have lower $Al_2O_3$ contents, ranging from 9.0 to 14.5 wt.% (Table 2). In addition, the garnet amphibolite samples do not have a marked depletion in CaO or $Na_2O$, with values ranging from 7.5 to 10.1 wt.% and 1.1 to 2.8 wt.%, respectively. The MgO content of the garnet amphibolite samples is notably less than in the gedrite samples, ranging from 6.0 to 11.2 wt.%, and enrichments are observed in $Fe_2O_3$, MnO, and $TiO_2$.

On an AFM diagram (Fig. 5), the gedrite-bearing samples are more aluminous and define a tighter cluster of values compared to the garnet amphibolite samples. On the ACF diagram (Fig. 6a), the cordierite–gedrite rocks dominantly plot along the A–F tieline, reflecting this low CaO content and limited amount of plagioclase. The garnet amphibolite samples plot more centrally in the diagram, reflecting the presence of a greater amount of plagioclase. Extreme depletion of K in the cordierite–gedrite rocks is reflected in the AKF diagram (Fig. 6b), with samples plotting along the A–F line, whereas most of the garnet amphibolite samples plot near or below the F apex, reflecting the plagioclase–orthoamphibole join.

Trace-element signatures of the cordierite–gedrite rocks display depletions in many low-field-strength elements (LFSE; field-strength elements as defined by

Saunders *et al*. 1980) including Ba and Sr (Table 2). Samples are enriched in many high-field-strength elements (HFSE) such as Zr, Hf, Nb and Ta. In addition, the samples show enrichments in the transition elements Cr, Ni, V, and Zn. In general, the garnet amphibolite samples show the same trace-element trends and variation in concentrations as the cordierite–gedrite rocks (Table 2).

TABLE 1. DESCRIPTION AND LOCATION OF GEOCHEMICAL AND GEOCHRONOLOGICAL SAMPLES FROM THOR-ODIN DOME, MONASHEE COMPLEX, BRITISH COLUMBIA

| Sample | Easting | Northing | Sample description | Location |
|---|---|---|---|---|
| AH-03-14 | 418667 | 5598701 | Grt-Crd-Ged rock | Bearpaw Lake |
| AH-03-15 | 418472 | 5598934 | Sil-Crd-Grt-Ged rock | Bearpaw Lake |
| AH-03-16 | 418563 | 5599096 | Sil-Crd-Grt-Ged rock | Bearpaw Lake |
| AH-03-23 | 419192 | 5599189 | Crd-Ged rock | Bearpaw Lake |
| AH-03-25 | 418836 | 5598004 | Grt-Crd-Ged rock | Bearpaw Lake |
| AH-03-26 | 418513 | 5598418 | Sil-Grt-Crd-Ged rock | Bearpaw Lake |
| AH-03-24 | 418812 | 5598068 | Grt amphibolite | Bearpaw Lake |
| AH-03-29 | 418497 | 5598511 | Grt amphibolite | Bearpaw Lake |
| AH-02-03 | 423426 | 5600049 | Grt amphibolite | Frigg Glacier |
| AH-02-04 | 423299 | 5600302 | Grt amphibolite | Frigg Glacier |

UTM locations are NAD83 and zone 11. Mineral symbols are from Kretz (1983).

The chondrite-normalized rare-earth-element (REE) patterns of the cordierite–gedrite samples are relatively flat, with $La_{(N)}/Yb_{(N)}$ values between 1 and 16 (Fig. 7a). The samples all have a slightly negative Eu anomaly. The garnet amphibolite samples have similar flat chondrite-normalized REE patterns, with $La_{(N)}/Yb_{(N)}$ values between 0.5 and 7 (Fig. 7b). On a primitive-mantle-normalized spider diagram, the cordierite–gedrite samples exhibit marked depletions in K, Ba and Sr, and enrichments in Cs, Th, U and the heavy rare-earth elements (HREE; Fig. 7c). The samples of garnet amphibolite also show the same general pattern of enrichments and depletions in these elements, with the exception that they lack the Th enrichment and the extreme degree of Sr depletion of the gedrite-bearing samples (Fig. 7c).

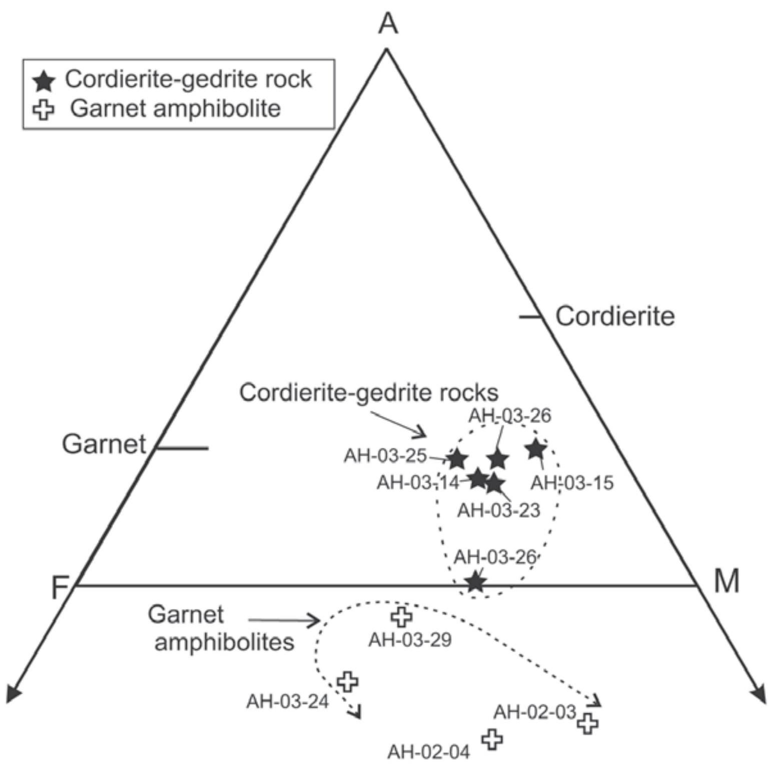


FIG. 5. An AFM diagram for the garnet amphibolite and cordierite–gedrite samples from the Thor–Odin dome. The parameters are (in mole percent, with total iron as FeO): A= $Al_2O_3$–CaO–$K_2O$–$Na_2O$ + 3.33*$P_2O_5$; F = FeO + MnO + $TiO_2$; M = MgO. Two of the garnet amphibolite samples plot outside the projection; the direction of their location is highlighted with the dashed arrow line.

TABLE 2. THE COMPOSITION OF GARNET AMPHIBOLITE AND CORDIERITE–GEDRITE SAMPLES FROM THOR–ODIN DOME, MONASHEE COMPLEX, BRITISH COLUMBIA

| | Cordierite–gedrite rock | | | | | | Garnet amphibolite | | | |
|---|---|---|---|---|---|---|---|---|---|---|
| | AH-03 -14 | AH-03 -15 | AH-03 -16 | AH-03 -23 | AH-03 -25 | AH-03 -26 | AH-03 -24 | AH-03 -29 | AH-02 -03 | AH-02 -04 |
| $SiO_2$ wt% | 40.52 | 53.10 | 45.14 | 62.31 | 28.11 | 50.85 | 49.39 | 50.96 | 46.59 | 45.91 |
| $TiO_2$ | 3.15 | 0.31 | 3.65 | 0.63 | 3.36 | 2.29 | 1.95 | 1.74 | 3.63 | 1.27 |
| $Al_2O_3$ | 17.78 | 20.01 | 12.98 | 12.75 | 23.07 | 15.76 | 13.23 | 14.48 | 9.00 | 13.40 |
| $Fe_2O_3$* | 3.64 | 1.55 | 3.94 | 2.33 | 3.50 | 2.24 | 4.30 | 3.70 | 3.99 | 4.93 |
| FeO | 11.99 | 4.27 | 11.36 | 7.02 | 17.15 | 8.21 | 11.70 | 10.41 | 9.60 | 11.32 |
| MnO | 0.11 | 0.08 | 0.19 | 0.19 | 0.25 | 0.11 | 0.24 | 0.24 | 0.17 | 0.22 |
| MgO | 18.09 | 16.54 | 12.53 | 12.35 | 18.87 | 13.60 | 5.96 | 7.97 | 11.19 | 6.83 |
| CaO | 0.99 | 0.21 | 5.96 | 0.37 | 2.04 | 1.07 | 10.12 | 7.53 | 8.96 | 9.55 |
| $Na_2O$ | 0.89 | 0.23 | 0.66 | 0.75 | 0.15 | 0.45 | 1.99 | 1.73 | 1.08 | 2.57 |
| $K_2O$ | 0.88 | 2.05 | 1.76 | 0.34 | 0.02 | 0.02 | 0.59 | 0.51 | 2.59 | 1.50 |
| $P_2O_5$ | 0.74 | 0.12 | 0.45 | 0.10 | 1.48 | 0.74 | 0.20 | 0.20 | 0.39 | 0.05 |
| Sum | 98.78 | 98.48 | 98.63 | 99.14 | 97.99 | 95.33 | 99.66 | 99.47 | 97.18 | 97.54 |
| V ppm | 334 | 25 | 306 | 156 | 451 | 200 | 345 | 329 | 283 | 264 |
| Cr | 104 | 92 | 685 | 421 | 205 | 32 | 206 | 254 | 840 | 352 |
| Co | 53 | 15 | 52 | 43 | 62 | 31 | 46 | 47 | 60 | 60 |
| Ni | 135 | 28 | 139 | 304 | 105 | 31 | 58 | 145 | 326 | 183 |
| Zn | 106 | 55 | 162 | 83 | 198 | 75 | 121 | 91 | 122 | 127 |
| Ga | 34 | 18 | 23 | 21 | 42 | 28 | 19 | 17 | 16 | 11 |
| As | <L.D. | <L.D. | <L.D. | <L.D. | <L.D. | <L.D. | <L.D. | <L.D. | <L.D. | <L.D. |
| Rb | 29.67 | 63.64 | 59.84 | 17.45 | 1.52 | 1.66 | 15.82 | 16.19 | 117.46 | 27.45 |
| Sr | 7.1 | 5.1 | 38.2 | 11 | 9.5 | 11 | 114.4 | 118.8 | 225.14 | 87.74 |
| Y | 34.97 | 19.5 | 33.12 | 27.17 | 108.95 | 47.66 | 37.87 | 32.6 | 37.11 | 30.24 |
| Zr | 263.9 | 164.8 | 189.7 | 57.5 | 242.6 | 226.9 | 114.9 | 100.9 | 160.09 | 45.13 |
| Nb | 13.3 | 13.2 | 22.4 | 7.0 | 14.9 | 10.1 | 10.2 | 8.2 | 18.7 | 1.53 |
| Cs | 0.79 | 0.73 | 1.41 | 0.93 | 0.15 | 0.09 | 0.15 | 0.82 | 5.00 | 0.50 |
| Ba | 6 | 80 | 87 | 67 | 9 | 9 | 139 | 10 | 271 | 59 |
| La | 31.55 | 34.95 | 38.80 | 14.80 | 19.14 | 37.92 | 15.28 | 9.00 | 24.34 | 2.09 |
| Ce | 67.40 | 71.62 | 88.38 | 31.86 | 45.97 | 74.04 | 36.19 | 22.63 | 60.47 | 5.83 |
| Pr | 8.10 | 7.71 | 11.65 | 3.74 | 6.46 | 8.19 | 4.86 | 3.21 | 9.74 | 1.08 |
| Nd | 32.56 | 26.68 | 51.57 | 14.85 | 30.58 | 31.33 | 21.90 | 15.62 | 43.89 | 6.18 |
| Sm | 5.86 | 4.59 | 10.81 | 3.10 | 9.10 | 6.37 | 5.61 | 4.37 | 10.95 | 2.80 |
| Eu | 1.21 | 0.63 | 3.43 | 0.63 | 2.82 | 1.46 | 1.60 | 1.80 | 4.40 | 1.22 |
| Gd | 5.97 | 3.92 | 9.45 | 3.48 | 15.04 | 9.02 | 6.52 | 5.48 | 11.00 | 4.49 |
| Tb | 0.96 | 0.64 | 1.31 | 0.62 | 2.93 | 1.51 | 1.10 | 0.94 | 1.67 | 0.89 |
| Dy | 5.90 | 3.75 | 7.03 | 4.22 | 19.47 | 8.95 | 6.89 | 5.85 | 7.86 | 5.27 |
| Ho | 1.29 | 0.70 | 1.30 | 0.92 | 4.08 | 1.73 | 1.45 | 1.22 | 1.49 | 1.17 |
| Er | 3.92 | 1.87 | 3.43 | 2.77 | 11.87 | 4.67 | 4.21 | 3.55 | 3.44 | 3.04 |
| Tm | 0.60 | 0.25 | 0.45 | 0.40 | 1.74 | 0.65 | 0.62 | 0.51 | 0.49 | 0.47 |
| Yb | 4.06 | 1.58 | 2.79 | 2.54 | 11.56 | 4.29 | 4.00 | 3.33 | 2.63 | 2.73 |
| Lu | 0.67 | 0.23 | 0.39 | 0.37 | 1.83 | 0.69 | 0.61 | 0.51 | 0.39 | 0.44 |
| Hf | 6.20 | 5.00 | 4.90 | 1.60 | 5.60 | 5.30 | 3.20 | 2.70 | 4.59 | 1.66 |
| Ta | 0.58 | 1.38 | 1.33 | 0.47 | 0.65 | 0.46 | 0.63 | 0.49 | 0.97 | <L.D. |
| Pb | 7.0 | 8.0 | 8.0 | <L.D. | 5.0 | 6.0 | <L.D. | 1.0 | 5.0 | 6.0 |
| Th | 3.01 | 47.78 | 5.36 | 4.42 | 1.79 | 2.06 | 2.23 | 1.04 | 2.75 | 0.40 |
| U | 5.42 | 9.37 | 1.10 | 1.56 | 4.97 | 3.87 | 0.59 | 0.55 | 0.84 | 0.82 |
| La/Th | 10.48 | 0.73 | 7.24 | 3.35 | 10.69 | 18.41 | 6.85 | 8.65 | 8.85 | 5.23 |

Major-element analyses were done by X-Ray Fluorescence. The proportions of $Fe_2O_3$* and FeO are recalculated from measured values of $Fe_2O_3T$ (total) using the procedure of LeMaitre (1976). Oxides normalized to 100% (anhydrous). Trace-element concentrations were established by X-ray fluorescence and inductively coupled plasma – mass spectrometry. <L.D.; less than the limit of detection.

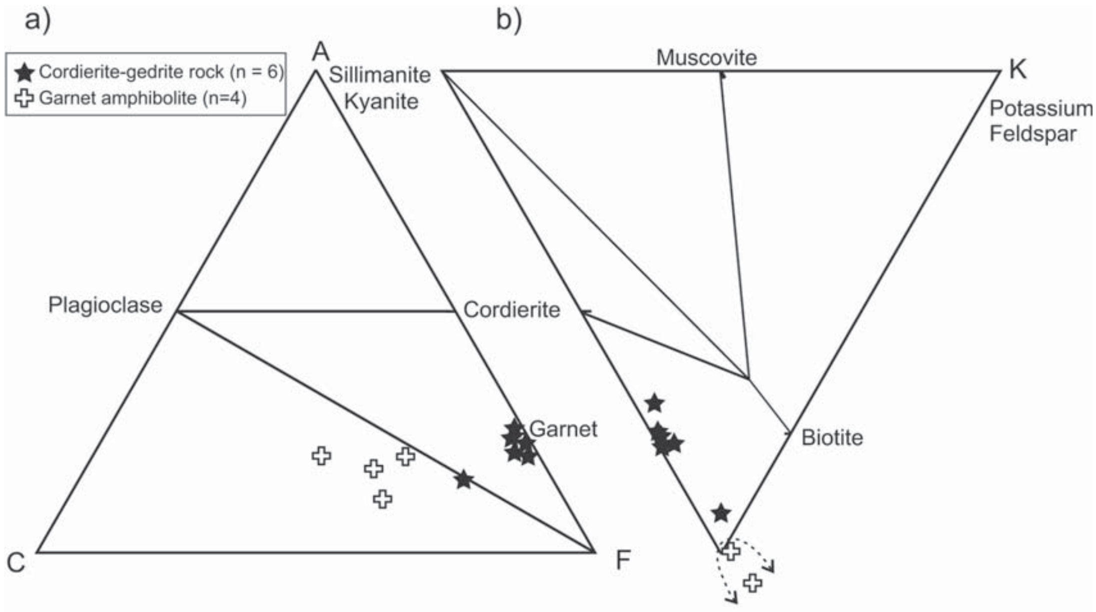


FIG. 6. Projections for the garnet amphibolite and cordierite–gedrite samples from the Thor–Odin dome. The parameters are in mole percent, and total iron is plotted as FeO. (a) An ACF diagram, with the following parameters: A = $Al_2O_3$ – $K_2O$; C = CaO + $Na_2O$ – 3.33*$P_2O_5$; F = FeO + MnO + MgO – $TiO_2$. (b) An AKF diagram, with the following parameters: A = $Al_2O_3$ – CaO – $Na_2O$ – 3.33*$P_2O_5$; K = $K_2O$; F = FeO + MnO + MgO – $TiO_2$.

*Whole-rock radiogenic isotope geochemistry*

Rubidium–strontium and samarium–neodymium data for whole-rock samples from the Bearpaw Lake area are presented in Table 3. Analytical methods are given in Appendix A. Three samples of cordierite–gedrite rock and three samples of garnet amphibolite were analyzed. Two samples each of the basement paragneiss and the basement orthogneiss are plotted (Fig. 8) for comparison (data from Hinchey & Carr 2006).

The cordierite–gedrite rocks have a range of $^{87}Sr/^{86}Sr$ values from 0.74923 to 0.85962, and $^{87}Rb/^{86}Sr$ values from 0.44 to 12.24. The garnet amphibolite samples have a range of $^{87}Sr/^{86}Sr$ values from 0.70953 to 0.74319, and $^{87}Rb/^{86}Sr$ values from 0.40 to 1.51. The four basement samples have a range of $^{87}Sr/^{86}Sr$ values from 0.72418 to 0.75236, and $^{87}Rb/^{86}Sr$ values from 0.80 to 1.79 (Hinchey & Carr 2006). The Sr data demonstrate the highly radiogenic nature of the Paleoproterozoic basement gneisses of the Thor–Odin area.

The primitive mantle has a present-day $^{87}Sr/^{86}Sr$ value of 0.7045 and the bulk silicate Earth has a $^{87}Rb/^{86}Sr$ value of 0.089. The Sr data for both the garnet amphibolite and the cordierite–gedrite rocks have a wide range of radiogenic values (Fig. 8). Data for basement gneisses and amphibolites from Parkinson (1991, 1992) are plotted for comparison (Fig. 8). The Rb–Sr isotope system appears to have been disturbed, likely during Cordilleran metamorphism, and therefore the data cannot be used to determine the protolith composition of the garnet amphibolite or cordierite–gedrite rocks.

The garnet amphibolite and cordierite–gedrite samples have distinct Nd isotopic compositions (Table 3). The cordierite–gedrite samples display a range in $^{147}Sm/^{144}Nd$ values, from 0.1084 to 0.1224, $\varepsilon Nd_{(today)}$ values from –15.3 to –20.6, and Nd model ages from $T_{(DM)}$ = 2.2 to 3.5 Ga. The garnet amphibolite samples have a range in $^{147}Sm/^{144}Nd$ values from 0.1502 to 0.1685, $\varepsilon Nd_{(today)}$ values from –0.8 to –7.3, and Nd model ages from $T_{(DM)}$ = 1.3 to 2.2 Ga. The four basement gneiss samples have a range in $^{147}Sm/^{144}Nd$ values from 0.0895 to 0.1176, and $\varepsilon Nd_{(today)}$ values from –20.4 to –27.4 (Hinchey & Carr 2006). Data for the basement gneiss and garnet amphibolite samples from Parkinson (1991, 1992) are plotted for comparison (Fig. 9). The $\varepsilon$Nd value is calculated at 760 Ma as a means of comparison, as this is likely the lower age constraint on the garnet amphibolite (see above). The samples are likely older, on the basis of lithological constraints (*i.e.,* the restricted occurrence of the cordierite–gedrite rocks in basement paragneiss) and Nd model ages. The rocks appear to have retained their original Sm and Nd isotopic signature, since the garnet amphibolite and cordierite–gedrite samples each plot as distinct homogeneous groups (Fig. 9). There is no evidence of differential mobility of Sm and Nd in the REE chemistry (Fig. 7). The differences in εNd signatures between the garnet amphibolite and cordierite–gedrite samples are, thus, likely inherited and not a result of metasomatism during Cordilleran metamorphism.

The data for the garnet amphibolite from both this investigation and Parkinson's study (1992) define a group with $\varepsilon Nd_{(760\ Ma)}$ values ranging from –0.3 to –4.6, suggesting only a limited interaction with crustal material. The cordierite–gedrite samples fall outside this group and appear to mirror the isotopic systematics of the basement gneiss (Fig. 9). The variation in Nd systematics between the cordierite–gedrite and amphibolite samples may be due to: a) Precambrian metamorphic alteration, b) a difference in age, c) alteration by fluids, or d) a primary feature of crustal contamination. The implications of each will be discussed below.

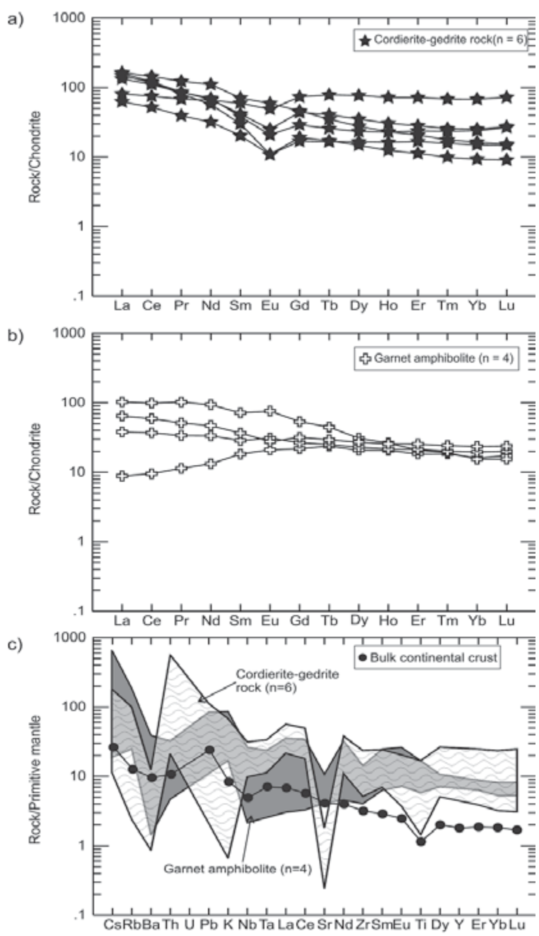


FIG. 7. Trace-element normalized diagrams. (a) Chondrite-normalized diagram for the cordierite–gedrite samples. (b) Chondrite-normalized diagram for the garnet amphibolite. (c) Primitive-mantle-normalized diagram for the range of cordierite–gedrite and garnet amphibolite samples. Normalization is from Sun & McDonough (1989). Data concerning the average bulk continental crust are taken from Taylor & McLennan (1995).

## DISCUSSION: INTERPRETATION OF PROTOLITH COMPOSITION

### *The cordierite–gedrite rocks*

The major-element composition of the cordierite–gedrite rocks may reflect either: a) an original protolith composition, or b) a protolith having undergone element mobilization, before or during metamorphism. It is not possible to distinguish between these two processes using the major-element composition, and therefore, these data only provide limited constraints on the protolith composition. Certain trace-elements, particularly the HFSE and transition elements, are generally considered relatively immobile during most secondary processes, and thus are more resistant to secondary alteration (Jenner 1996). These elements are therefore more likely to reflect primary protolith composition. The low abundance of LFSE such as K, Sr, and Ba suggests that these mobile elements have been affected by secondary alteration. This interpretation is supported by the Sr isotopic signatures, which also are disturbed.

The cordierite–gedrite rocks show general systematic variations between most immobile trace-element concentrations and silica weight percent, indicating that these elements were not adversely affected by alteration (Figs. 10a, b). On the Th–Hf–Co diagram of Taylor & McLennan (1985), most of the cordierite–gedrite samples plot close to the Co apex (Fig. 11). The Th/Hf value in most rock types (igneous, sedimentary or metamorphic) varies little, and therefore most crustal materials plot along a linear array. Mafic material generally plots close to the Co apex, and more felsic material plots toward the opposite side of the diagram. The cordierite–gedrite rocks have an average Th/Hf value of 2.4, which is interpreted to reflect a primary mafic composition. In addition, the flat REE patterns and slightly negative Eu anomaly are consistent with basaltic to andesitic signatures (Taylor & McLennan 1985, Rollinson 1993). On the tectonic discrimination diagram $Zr/TiO_2$ *versus* Nb/Y, the cordierite–gedrite samples mostly fall in the andesite to basalt field, with one sample falling in the rhyolite field (Fig. 12). The major- and trace-element composition of the cordierite–gedrite rocks indicate that they are likely altered mafic volcanic rocks.

TABLE 3. WHOLE-ROCK Sr AND Nd ISOTOPE DATA OF THE CORDIERITE–GEDRITE ROCKS AND GARNET AMPHIBOLITE FROM THE THOR–ODIN DOME, MONASHEE COMPLEX, BRITISH COLUMBIA

| Sample no. | Rb ppm | Sr ppm | $^{87}$Sr/$^{86}$Sr meas.[a, b] | 2σ[d] ± | $^{87}$Rb/$^{86}$Sr calc.[c] | $^{87}$Sr/$^{86}$Sr 760 Ma | Sm ppm | Nd ppm | $^{143}$Nd/$^{144}$Nd meas.[a, b] | 2σ[d] ± | $^{147}$Sm/$^{144}$Nd calc.[c] | $^{143}$Nd/$^{144}$Nd 760 Ma | εNd[e] 760 Ma | $T_{DM}$[f] Ma |
|---|---|---|---|---|---|---|---|---|---|---|---|---|---|---|
| AH-03-14 BL Grt-Crd-Ged rock | 29.6 | 7.1 | 0.859617 | 15 | 12.242 | 0.72679 | 5.86 | 32.56 | 0.511583 | 13 | 0.10838 | 0.51104 | -12.0 | 2259 |
| AH-03-25 BL Grt-Crd-Ged rock | 1.52 | 9.5 | 0.771449 | 24 | 0.466 | 0.76639 | 9.1 | 30.58 | 0.511853 | 14 | 0.17920 | 0.51096 | -13.6 | 3495 |
| AH-03-26 BL Sil-Grt-Crd-Ged rock | 1.66 | 11 | 0.749230 | 28 | 0.438 | 0.74447 | 6.37 | 31.33 | 0.511635 | 24 | 0.12244 | 0.51102 | -12.4 | 2517 |
| AH-03-24 BL Grt amphibolite | 15.82 | 114.4 | 0.718968 | 47 | 0.401 | 0.71462 | 5.61 | 21.9 | 0.512262 | 14 | 0.15426 | 0.51149 | -3.2 | 2263 |
| AH-03-29 BL Grt amphibolite | 16.19 | 118.8 | 0.743187 | 24 | 0.396 | 0.73889 | 4.37 | 15.62 | 0.512583 | 11 | 0.16847 | 0.51174 | 1.7 | 1898 |
| AH-02-03 FG Grt amphibolite | 117.46 | 225.14 | 0.709529 | 15 | 1.510 | 0.69315 | 10.95 | 43.89 | 0.512598 | 10 | 0.15024 | 0.51185 | 3.7 | 1322 |

[a] Measurements by TIMS. [b] Measured and corrected for mass fractionation. [c] Calculated using ppm concentrations from ICP–MS trace-element analysis. [d] Errors refer to last one or two digits and are propagated to include reproducibility of standard analysis and run errors. [e] Calculated using present-day chondritic uniform reservoir with $^{143}$Nd/$^{144}$Nd = 0.512638 and $^{147}$Sm/$^{144}$Nd = 0.1967. [f] Depleted mantle model age, assuming a $^{147}$Sm/$^{144}$Nd value for depleted mantle (DM) of 0.214 and a present-day $^{143}$Nd/$^{144}$Nd value of 0.513115. Location: BL: Bearpaw Lake, FG: Frigg Glacier.

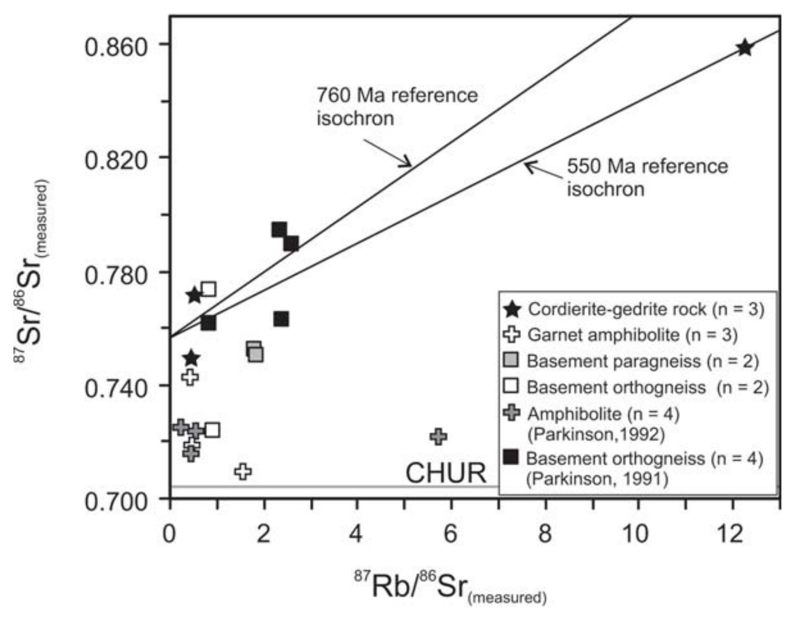


FIG. 8. $^{87}$Rb/$^{86}$Sr$_{(measured)}$ *versus* $^{87}$Sr/$^{86}$Sr$_{(measured)}$ diagram for the cordierite–gedrite rocks, garnet amphibolite and selected samples of basement gneiss for comparison. Basement orthogneiss and amphibolite from Parkinson (1991, 1992, respectively) are plotted for comparison. CHUR: chondritic uniform reservoir.

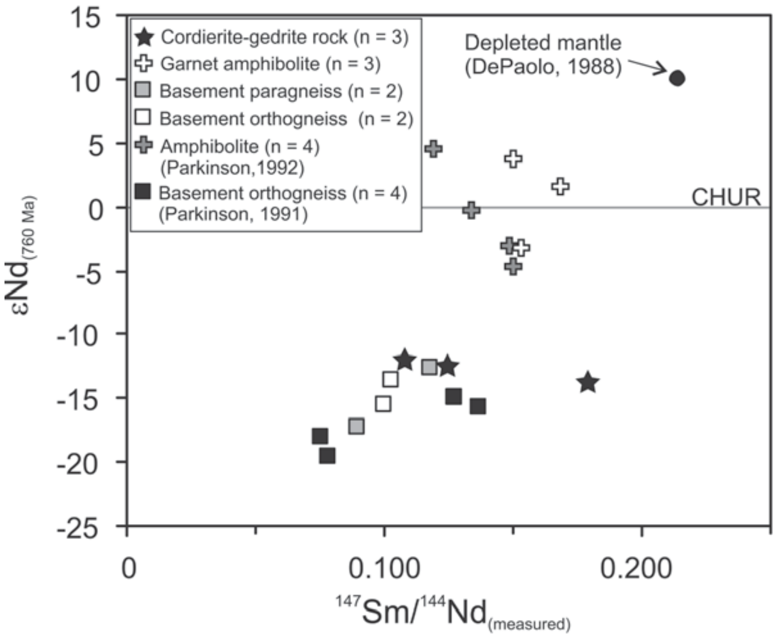


FIG. 9. $^{147}Sm/^{144}Nd_{(measured)}$ *versus* $\varepsilon Nd_{(760\ Ma)}$ diagram for the cordierite–gedrite rocks, garnet amphibolite and selected samples of basement gneiss for comparison. Basement orthogneiss and amphibolite from Parkinson (1991, 1992, respectively) are plotted for comparison. Depleted mantle from DePaolo (1988) is plotted. CHUR: chondritic uniform reservoir.

The variable Nd isotopic signature of the cordierite–gedrite rocks may be interpreted several ways. Either a) the isotope system was affected by metasomatism resulting in the preferential mobility of the parent or daughter element, or b) the signature is primary, and the product of either significant crustal contamination or a heterogeneous source. On the basis of trace-element enrichments, the cordierite–gedrite rocks are interpreted to be mafic or intermediate volcanic rocks. There does not appear to be any significant fractionation of Sm and Nd. The Nd isotopic values could therefore be primary, and the range in values could represent minor crustal contamination, although minor alteration cannot be precluded.

*The garnet amphibolite*

The garnet amphibolite samples have a basaltic composition (Table 2). In terms of the major and trace elements, the rocks are similar to modern basaltic rocks (Rollinson 1993). The amphibolite samples dominantly plot in the basalt field on the Nb/Y *versus* $Zr/TiO_2$ diagram (Fig. 12). These data suggest that the amphibolite rocks are the metamorphic equivalent of basalts, and that high-grade Late Cretaceous to Eocene metamorphism had little effect on their chemical composition. This conclusion is supported by the high average Cr/Th value, 380, and the high average La/Th value, 7.4. These values are different from those of typical sedimentary rocks, which have Cr/Th = 7.5 and La/Th = 2.6 (Taylor & McLennan 1985), but are typical for mafic magmatic rocks (Rollinson 1993). The interpretation of a mafic protolith is further supported by the high MgO and $TiO_2$ values, and general major-element trends (Table 2).

The amphibolite samples have a flat REE pattern; the lack of a HREE depletion suggests that the primitive melt either formed a) at a shallow depth in the mantle, outside the stability field of garnet, or b) by high degrees of partial melting (Fig. 7b). Although the LFSE are fractionated with respect to HFSE (Fig. 7c), some of the LFSE may have been remobilized during metamorphism, and therefore caution must be exercised in interpreting igneous evolution using these elements. The trace-element signatures suggest that the garnet amphibolite samples had either a source influenced by an enriched mantle, or protolith melts that were contaminated by a minor amount of crust.

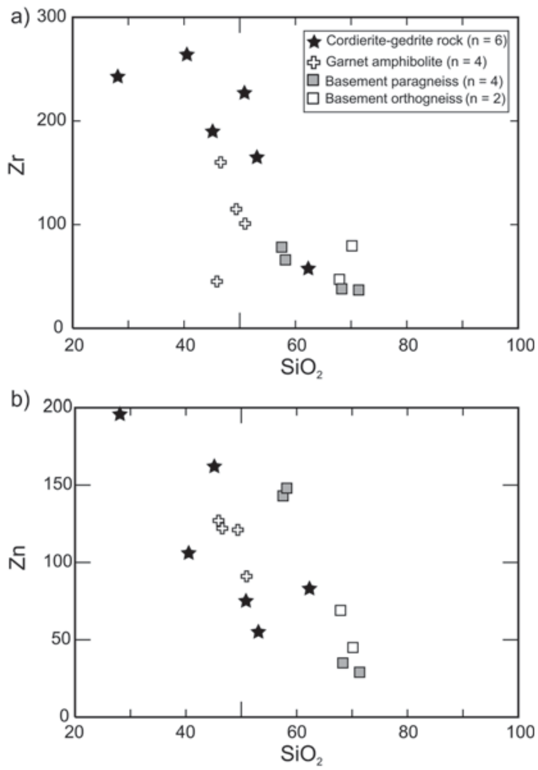


The garnet amphibolite samples have a more primitive Nd isotopic signature than the cordierite–gedrite rocks. The signatures can be interpreted in several ways: a) the signatures are primary, and reflect the model age of extrusion or emplacement, presumably only slightly affected by crustal contamination, or b) the system was affected by secondary alteration, which did not disturb these rocks as extensively as it may have disturbed the cordierite–gedrite rocks. The lack of a notable disturbance in the trace-element signatures indicates that alteration was likely not a significant process. Therefore, the Nd isotopic values are interpreted to be primary in origin. The $T_{DM}$ model ages range from 1.3 to 2.2 Ga, supporting a Precambrian age of the rocks. The range in values may reflect: a) minor contamination by crust during emplacement, or b) inclusion of more than one suite of volcanic rocks or mafic dykes in the garnet amphibolite suite.

FIG. 10. $SiO_2$ *versus* (a) Zr, and (b) Zn in the garnet amphibolite, cordierite–gedrite rocks and selected samples of basement gneiss from the Thor–Odin dome.

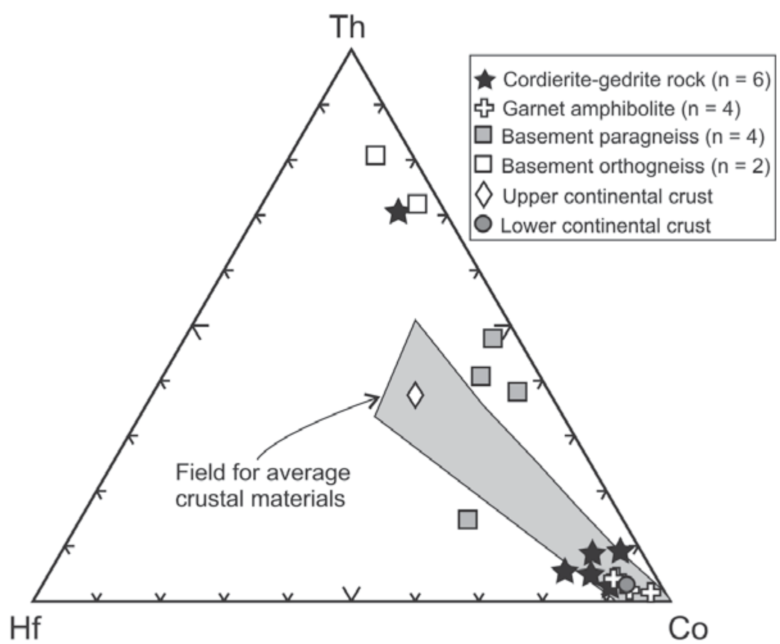


FIG. 11. Plot of Hf–Th–Co data from the garnet amphibolite, cordierite–gedrite rocks, and selected samples of basement gneiss. Average upper and lower continental crust and the field for average crustal material are from Taylor & McLennan (1985).

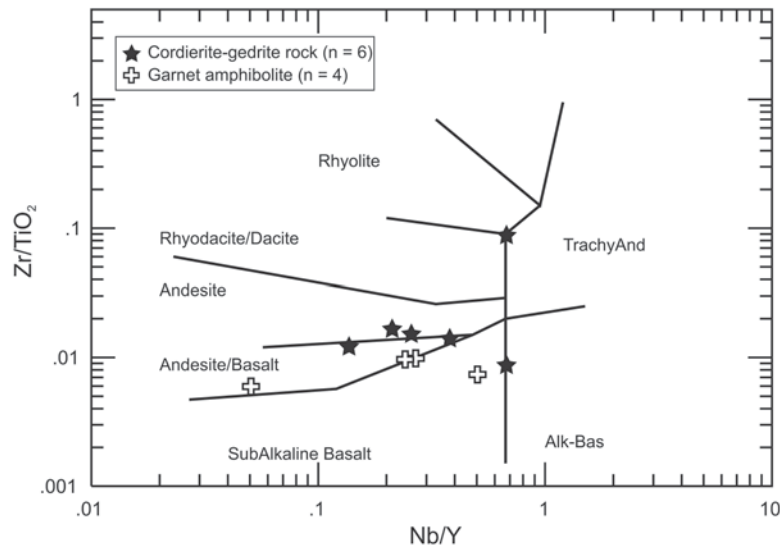


FIG. 12. A plot of Nb/Y *versus* $Zr/TiO_2$ for garnet amphibolite and cordierite–gedrite samples. Fields of volcanic rocks are from Winchester & Floyd (1977).

## DISCUSSION: GENETIC MODELS FOR THE CORDIERITE–GEDRITE ROCKS

The cordierite–gedrite rocks in the Thor–Odin dome are most likely hydrothermally altered mafic volcanic rocks that were altered during or shortly after their formation in the Proterozoic. Hydrothermal alteration, by seawater, of volcanic rocks ranging from basalts to rhyolites will generally result in the loss of Ca and gain of Mg (Smith *et al*. 1992, Peck & Smith 2005). The effects of the alteration depend on several factors including, but not limited to, temperature of fluids, initial composition of the protolith, and water-to-rock ratio (Smith *et al*. 1992). The end result, however, is the equivalent of a "chlorite schist", and its subsequent prograde metamorphism could result in the spectrum of cordierite–orthoamphibole assemblages (Smith *et al*. 1992). This is consistent with most occurrences of these rocks, which are interpreted to have achieved their chemical composition before metamorphism (Spear & Schumacher 1982). The low concentration of Ca and relatively high concentration of Mg in the cordierite–gedrite rocks suggest that this process, followed by high-grade metamorphism, was significant in their petrogenesis. Hydrothermal fluids, likely seawater, would have had local access along faults, and thus fracture density would control the extent of hydrothermal alteration of a volcanic pile, providing a mechanism whereby altered volcanic rocks could easily be interlayered with unaltered rocks, a relationship commonly observed in the field (Spear & Schumacher 1982). If the garnet amphibolite samples were part of the same volcanic package as the cordierite–gedrite rocks, then this mechanism could explain partial preservation of the protolith of some original mafic rocks, which were metamorphosed to become garnet amphibolite, while others were altered, and the cordierite–gedrite rocks resulted. However, the difference in degree of alteration could also be explained if the garnet amphibolite rocks represent a younger suite of dykes, as suggested by the less evolved $\varepsilon$Nd signatures, Nd model ages, and occurrence throughout the domes, and if they formed after the cordierite–gedrite rocks were altered. Regardless, the cordierite–gedrite rocks of the Thor–Odin dome are interpreted as being hydrothermally altered prior to being metamorphosed at conditions of the upper amphibolite facies in the Late Cretaceous to Eocene during Cordilleran orogenesis.

Metasomatic processes during the Late Cretaceous to Eocene Cordilleran metamorphism are unlikely to have formed the cordierite–gedrite rocks of the Thor–Odin dome. The cordierite–gedrite rocks are part of a regionally metamorphosed, deformed and transposed basement complex, which does not contain a single, obvious source for metasomatic fluids. In addition, if metasomatism had occurred at that time, it would have affected other rocks, including the garnet amphibolite boudins, which would initially have had a similar protolith composition. If this were the case, then the occurrence of highly "altered" cordierite–gedrite rocks adjacent to garnet amphibolite would need to be explained. The role and extent of Precambrian metamorphism are uncertain in these rocks, and therefore the potential involvement of metasomatic fluids during the

Precambrian cannot be fully evaluated. It is reasonable to entertain a model whereby the rocks were altered in a seafloor setting shortly after, or during, their original formation.

The synmetamorphic model, in which the formation of these rocks is a byproduct or residuum of partial melting of a pelitic sediment or metavolcanic rock, is unlikely in this situation. The basement rocks of the Thor–Odin dome experienced partial melting between 56 and 51 Ma, and the onset of anatexis was concomitant with Late Cretaceous to Eocene peak metamorphism and continued during isothermal decompression (Vanderhaeghe *et al*. 1999, 2003, Teyssier *et al*. 2005, Hinchey 2005, Hinchey *et al*. 2006). If the cordierite–gedrite rocks are a residuum of partial melting, then the residuum would have formed during the Late Cretaceous to Eocene orogenic event and not prior to it. The coarse-grained textures, petrography, geochemistry and geochronology of the cordierite–gedrite rocks indicate that the metamorphic minerals grew and were modified at *ca*. 56 to 50 Ma, during Cordilleran metamorphism and decompression, and are not significantly older, as the preserved textures would not have survived a subsequent metamorphic event (Norlander *et al*. 2002, Hinchey 2005, Hinchey *et al*. 2006, 2007). Therefore, the chemical composition of these rocks must have been established prior to the Late Cretaceous to Eocene metamorphism and anatexis.

The paleoregolith model is unlikely for several reasons. Firstly, the weathering profiles in paleosols formed by the alteration of mafic volcanic rocks commonly have enrichments in residual Zr (Moore & Waters 1990, Gallet *et al*. 1996), with values typically in excess of ~690 ppm of Zr and levels as high as 10000 ppm (Degenhardt 1957). The cordierite–gedrite samples of this study do not fall in this range; rather, they contain 58–264 ppm of Zr, which is comparable to average continental crust values of 100 ppm (Taylor & McLennan 1985). Secondly, residual soils commonly show large enrichments in Ti (up to 30% $TiO_2$) and can show LREE enrichments, notably in Ce, if derived in humid climates (Moore & Waters 1990). The cordierite–gedrite rocks are not excessively enriched in Ti, and do not have a LREE enrichment or Ce anomaly. In addition, most paleosols have a nearly constant La/Th value of ~2.8, reflecting a homogenization of the crust (Gallet *et al*. 1996) similar to the post-Archean shale value (Taylor & McLennan 1985). The cordierite–gedrite samples have La/Th values ranging from 0.7 to 18.4, indicating that a paleosol or paleoregolith source is unlikely. On the basis of their chemical signatures, it seems unlikely that these rocks formed from the metamorphism of a paleosol or paleoregolith.

## Regional Correlation

Within the Thor–Odin dome and surrounding area, the cordierite–gedrite rocks are restricted to the southwestern portion of the Thor–Odin dome; however, amphibolite rocks are known to occur throughout the region. Correlations between amphibolite rocks of the Thor–Odin dome and the surrounding area can be considered. Occurrences of amphibolite are documented to the north of the Monashee complex and south of the Malton complex, where they are hosted by Proterozoic Windermere to Lower Paleozoic platformal strata (Simony *et al*. 1980, Monger *et al*. 1982, Sevigny 1988). These amphibolite rocks are interpreted as Late Proterozoic mantle-derived basalts on the basis of geochemistry (Sevigny 1988). In comparing the major- and trace-element composition of the amphibolite samples from Sevigny's (1988) study with those of this study, the signatures show considerable similarities. This includes enrichments in CaO and MgO, similar trace-element concentrations, and relatively flat REE concentrations. On the Zr/Nb *versus* $Ce_{(N)}/Sm_{(N)}$ diagram, all samples from both studies fall in a similar range (Fig. 13). The amphibolite samples from this study and those of Sevigny (1988) may thus represent one mafic suite; however, additional radiogenic isotope and U–Pb studies would be required to test whether these amphibolite rocks belong to one or more suites.

Other Proterozoic mafic volcanic suites in the southern Omineca belt include volcanic rocks of the Windermere Supergroup and mafic intrusions of the Belt–Purcell Supergroup (Frost & O'Nions 1984, Frost & Winston 1987, Burwash *et al*. 1988, Burwash & Wagner 1989, Devlin *et al*. 1988, Sevigny & Thériault 2003). The Nd isotopic signatures of mafic suites hosted by these two supergroups are compared with the garnet amphibolite and cordierite–gedrite rocks from the Thor–Odin dome, to evaluate whether or not correlations may be permissible (Fig. 14). Samples of Eocene lamprophyre dykes, exposed south of the Valhalla complex and from the Three Valley suite from the northern Thor–Odin dome, also have been plotted for comparison (Figs. 12, 14), as these rocks have distinct chemical and Nd isotopic signatures (Sevigny & Thériault 2003, Adams *et al*. 2005).

The Nd isotopic signatures of the garnet amphibolite and cordierite–gedrite samples plot distinctly into two broad groups (Fig. 14). When compared with the Nd isotopic signatures of the volcanic mafic rocks of the Horsethief Creek Group and the Moyie sills (Fig. 14), the samples from the Thor–Odin garnet amphibolite and cordierite–gedrite rocks broadly overlap and do not fall entirely into either domain. The samples partially overlap with both fields of the volcanic suites of Horsethief Creek Group and the Moyie sills (Fig. 14), but show different trends; therefore the Nd isotopic data cannot form the basis for a positive correlation with either mafic suite.

The garnet amphibolite boudin dated by Parkinson (1992) from the Middle Crustal Zone rocks, near Three Valley Gap, which gave a poorly constrained upper intercept age of 1571 ± 76 Ma, is the only sample of this

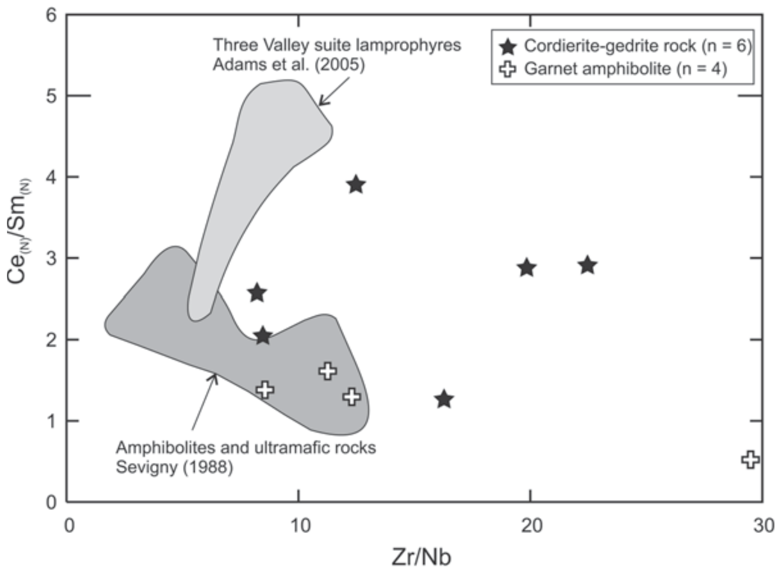


FIG. 13. Comparison of Zr/Nb *versus* $Ce_{(N)}/Sm_{(N)}$ for garnet amphibolite and cordierite–gedrite rocks from this study. For comparison, fields are plotted for amphibolites from south of the Malton complex (data from Sevigny 1988) and lamprophyres of the Three Valley suite from the northern part of the Thor–Odin dome (data from Adams *et al.* 2005). Normalization values are from Sun & McDonough (1989).

lithology for which a U–Pb age date is available. The Nd isotopic data for this sample indicate an $\varepsilon Nd_{(760 Ma)}$ of –6.1 and a $T_{(DM)}$ age of 2.6 Ga. Parkinson interpreted this sample as likely being correlative with the 1.45 Ga Moyie sills (Höy 1989). The isotopic signature overlaps with some garnet amphibolite samples exposed in the basement gneiss of the Thor–Odin dome and in part overlaps with the Moyie sills (Fig. 14). Some of the garnet amphibolite samples may, at least in part, represent this *ca.* 1.5 Ga suite, although the scatter in the data precludes a conclusive correlation. On the basis of the present dataset, neither the cordierite–gedrite rocks nor the garnet amphibolite can be distinguished from other Proterozoic mafic suites known to have intruded the southern Omineca belt. However, the garnet amphibolite samples clearly do not correlate with the Eocene lamprophyre dykes, as the lamprophyres have a less evolved Nd isotopic signatures, are weakly altered, are *ca.* 50 Ma, and intruded into the Omineca belt following the onset of extension (Sevigny & Thériault 2003, Adams *et al.* 2005).

## SUMMARY OF CONCLUSIONS

1) In the southwestern portion of the Thor–Odin dome, cordierite–gedrite rocks occur as discontinuous layers that are locally boudinaged, concordant with the pervasive $S_2$ transposition foliation, preserved on the limbs of $F_2$ isoclines, and appear to be a discontinuous marker-horizon or horizons within the basement paragneiss. In the Bearpaw Lake area, the cordierite–gedrite rocks are interlayered with garnet amphibolite boudins that also occur as discontinuous lenses parallel to the pervasive $S_2$ transposition foliation within the Paleoproterozoic basement paragneisses, are not observed cross-cutting the cordierite–gedrite rocks, yet are known to occur throughout the Thor–Odin dome area.

2) On the basis of field evidence, major- and trace-element signatures and Nd isotopic systematics, the cordierite–gedrite rocks are interpreted as lenses of Paleoproterozoic mafic volcanic rocks that are part of the basement gneiss of the Thor–Odin dome. The distinctive bulk-rock composition of the cordierite–gedrite rocks is interpreted to have resulted from hydrothermal alteration, likely by seawater.

3) On the basis of field evidence, major-element signatures, trace-element signatures and Nd isotopic signatures, the garnet amphibolite rocks are likely Proterozoic in age and are interpreted as metamorphosed mafic rocks that likely postdated the formation of the protolith of the cordierite–gedrite rocks.

4) Owing to significant overlap in the concentration of major elements, trace elements and the large range in Nd isotopic values of the cordierite–gedrite and amphibolite rocks relative to other mafic suites in the region, neither suite can be distinguished from

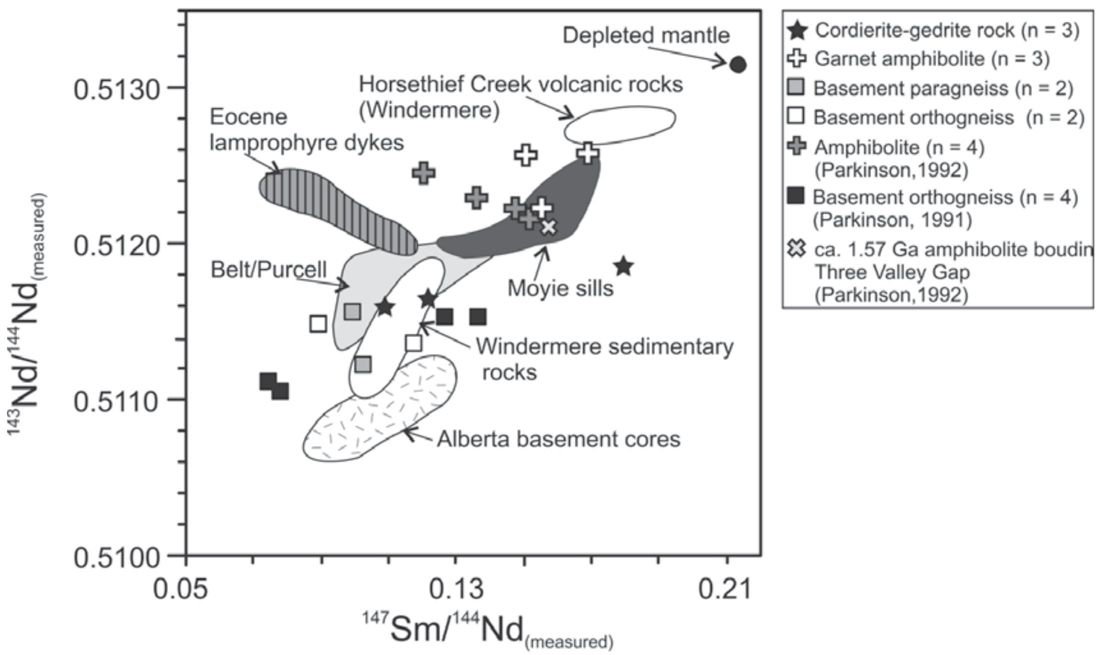


FIG. 14. $^{147}Sm/^{144}Nd_{(measured)}$ *versus* $^{143}Nd/^{144}Nd_{(measured)}$ diagram for the garnet amphibolite, cordierite–gedrite rocks and selected samples of basement gneiss from the Thor–Odin dome. Basement orthogneiss and amphibolite, from Parkinson (1991, 1992, respectively) are plotted for comparison. Data on Eocene lamprophyres are from Sevigny & Thériault (2003) and Adams *et al*. (2005). Isotopic data for the Paleoproterozoic supergroups (Windermere, Belt–Purcell) and Archean basement cores for the Canadian Cordillera are plotted for comparison. Data are from Frost & O'Nions (1984), Devlin *et al*. (1985), Frost & Burwash (1986), Frost & Winston (1987), Burwash *et al*. (1988), Devlin *et al*. (1988), Burwash & Wagner (1989), Ross *et al*. (1993), and Anderson & Goodfellow (2000). Depleted mantle values are from DePaolo (1988).

lithologically similar Proterozoic candidates such as the Moyie Sills of the Belt–Purcell Supergroup or volcanic rocks of the Horsethief Creek Group of the Windermere Supergroup.

## Acknowledgements

This contribution is part of the Ph.D. dissertation of AMH at Carleton University. Financing for this study was provided by a Natural Sciences and Engineering Research Council grant to SDC, a scholarship to AMH from Carleton University and an Ontario Graduate Scholarship. Paul McNeill is thanked many fruitful discussions in and out of the field. We thank many people at Carleton University for assistance, including B. Cousens and J. Blenkinsop for help with Sm–Nd and Rb–Sr analysis. Critical reviews by W.E. Trzcienski Jr. and Paul Glombick improved the clarity of the manuscript.

## References

ADAMS, M.G., LENTZ, D.R., SHAW, C.S.J., WILLIAMS, P.F., ARCHIBALD, D.A. & COUSENS, B. (2005): Eocene shoshonitic mafic dykes intruding the Monashee Complex, British Columbia: a petrogenetic relationship with the Kamloops Group volcanic sequence? *Can. J. Earth Sci*. **42**, 11-24.

ANDERSON, H.E. & GOODFELLOW, W.D. (2000): Geochemistry and isotope chemistry of the Moyie sills: implications for early tectonic setting of the Mesoproterozoic Purcell basin. *In* The Geological Environment of the Sullivan Pb–Zn–Ag Deposit (J.W. Lydon, T. Höy, J.F. Slack & M.E. Knapp, eds.). *Geol. Assoc. Can., Mineral Deposits Division, Spec. Publ*. **1**, 302-321.

BROWN, R.L. (2004): Thrust-belt accretion and hinterland underplating of orogenic wedges; an example from the Canadian Cordillera. *In* Thrust Tectonics and Hydrocarbon Systems (K.R. McClay, ed.). *Am. Assoc. Petroleum Geol., Mem*. **82**, 51-64.

Brown, R.L. & Gibson, H.D. (2006): An argument for channel flow in the southern Canadian Cordillera and comparison with Himalayan tectonics. *In* Channel Flow, Ductile Extrusion and Exhumation of Lower-Mid-Crust in Continental Collision Zones (R. Law, M. Searle & L. Godin, eds.). *Geol. Soc., Spec. Publ.* (in press).

Brown, R.L., Journey, J.M., Lane, L.S., Murphy, D.C. & Rees, C.J. (1986): Obduction, backfolding and piggyback thrusting in the metamorphic hinterland of the southeastern Canadian Cordillera. *J. Struct. Geol.* **8**, 225-268.

Burwash, R.A., Cavell, P.A. & Burwash, E.J. (1988): Source terranes for Proterozoic sedimentary rocks in southern British Columbia; Nd isotopic and petrographic evidence. *Can. J. Earth Sci.* **25**, 824-832.

Burwash, R.A. & Wagner, P.A. (1989): Sm/Nd geochronology of the Moyie Intrusions, Moyie Lake map area, British Columbia (82G/5). *In* Geological Fieldwork 1988; a Summary of Field Activities and Current Research. *British Columbia Ministry of Energy, Mines and Petroleum Resources Pap.* **1989-1**, 45-48.

Carr, S.D. (1991): Three crustal zones in the Thor–Odin–Pinnacles area, southern Omineca Belt, British Columbia. *Can. J. Earth Sci.* **28**, 2003-2023.

Carr, S.D. (1992): Tectonic setting and U–Pb geochronology of the early Tertiary Ladybird Leucogranite suite, Thor–Odin – Pinnacles area, southern Omineca belt, British Columbia. *Tectonics* **11**, 258-278.

Carr, S.D. & Simony, P.S. (2006): Ductile thrusting vs. channel flow in the southeastern Canadian Cordillera: evolution of a coherent crystalline thrust sheet. *In* Channel Flow, Ductile Extrusion and Exhumation of Lower-Mid-Crust in Continental Collision Zones (R. Law, M. Searle & L. Godin, eds.). *Geol. Soc., Spec. Publ.* (in press).

Coleman, V.J. (1990): *The Monashee Décollement at Cariboo Alp and Regional Kinematic Indicators, Southeastern British Columbia*. M.S. thesis, Carleton Univ., Ottawa, Ontario.

Crowley, J.L. (1999): U–Pb geochronological constraints on Paleozoic tectonism in the Monashee complex, Canadian Cordillera: elucidating an overprinted geologic history. *Geol. Soc. Am., Bull.* **111**, 560-577.

Crowley, J.L., Brown, R.L. & Parrish, R.R. (2001): Diachronous deformation and a strain gradient beneath the Selkirk allochthon, northern Monashee complex, southeastern Canadian Cordillera. *J. Struct. Geol.* **23**, 1103-1121.

Crowley, J.L. & Parrish, R.R. (1999): U–Pb isotopic constraints on diachronous metamorphism in the northern Monashee Complex, southern Canadian Cordillera. *J. Metam. Geol.* **17**, 483-502.

Degenhardt, H. (1957): Untersuchungen zur geochemischen Verteilung des Zirkoniums in der Lithosphaere. *Geochim. Cosmochim. Acta* **11**, 279-309.

DePaolo, D.J. (1988): *Neodymium Isotope Chemistry: an Introduction*. Springer-Verlag, New York, N.Y.

Devlin, W.J., Bond, G.C. & Brueckner, H.K. (1985): An assessment of the age and tectonic setting of volcanics near the base of the Windermere Supergroup in northeastern Washington; implications for latest Proterozoic – earliest Cambrian continental separation. *Can. J. Earth Sci.* **22**, 829-837.

Devlin, W.J., Brueckner, H.K. & Bond, G.C. (1988): New isotopic data and a preliminary age for volcanics near the base of the Windermere Supergroup, northeastern Washington, U.S.A. *Can. J. Earth Sci.* **25**, 1906-1911.

Duncan, I.J. (1982): *The Evolution of the Thor–Odin Gneiss Dome and Related Geochronological Studies*. Ph.D. thesis, Univ. British Columbia, Vancouver, B.C.

Duncan, I.J. (1984): Structural evolution of the Thor–Odin gneiss dome. *Tectonophysics* **101**, 87-130.

Eskola, P. (1914): On the petrology of the Orijarvi regional in southwestern Finland. *Bull. Comm. Géol. Finlande* **40**, 1-279.

Frost, C.D. & Burwash, R.A. (1986): Nd evidence for extensive Archean basement in the western Churchill Province, Canada. *Can. J. Earth Sci.* **23**, 1433-1437.

Frost, C.D. & O'Nions, R.K. (1984): Nd evidence for Proterozoic crustal development in the Belt–Purcell Supergroup. *Nature* **312**, 53-56.

Frost, C.D. & Winston, D. (1987): Nd isotope systematics of coarse- and fine-grained sediments; examples from the middle Proterozoic Belt–Purcell Supergroup. *J. Geol.* **95**, 309-327.

Gable, D.J. & Sims, P.K. (1969): Geology and regional metamorphism of some high-grade cordierite gneisses, Front Range, Colorado. *Geol. Soc. Am., Spec. Pap.* **128**, 87-???.

Gallet, S., Jahn, B. & Torii, M. (1996): Geochemical characterization of the Luochuan loess–paleosol sequence, China, and paleoclimatic implications. *Chem. Geol.* **133**, 67-88.

Gibson, H.D., Brown, R.L. & Parrish, R.R. (1999): Deformation-induced inverted metamorphic field gradients; an example from the southeastern Canadian Cordillera. *J. Struct. Geol.* **21**, 751-767.

Glombick, P.M. (2005): *Mesozoic to Early Tertiary Tectonic Evolution of the Shuswap Metamorphic Complex in the Vernon Area, Southeastern Canadian Cordillera*. Ph.D. thesis, Univ. of Alberta, Edmonton, Alberta.

Grant, J.A. (1968): Partial melting of common rocks as a possible source of cordierite–anthophyllite bearing assemblages. *Am. J. Sci.* **266**, 908-931.

Hinchey, A.M. (2005): *Thor–Odin Dome: Constraints on Paleocene–Eocene Anatexis and Deformation, Leucogran-*

*ite Generation and the Tectonic Evolution of the Southern Omineca Belt, Canadian Cordillera*. Ph.D. thesis, Carleton University, Ottawa, Ontario.

HINCHEY, A.M. & CARR, S.D. (2006): The S-type Ladybird leucogranite suite of southeastern British Columbia: geochemical and isotopic evidence for a genetic link with migmatite formation in the North American basement gneisses of the Monashee complex. *Lithos* **90**, 223-248.

HINCHEY, A.M., CARR, S.D., MCNEILL, P.D. & RAYNER, N. (2006): Paleocene-Eocene high-grade metamorphism, anatexis and deformation in Thor–Odin dome, Monashee complex, southeastern British Columbia. *Can. J. Earth Sci.* **43**, 1341-1365.

HINCHEY, A.M., CARR, S.D. & RAYNER, N. (2007): Bulk compositional controls on the preservation of age domains within metamorphic monazite: a case study from quartzite and garnet-cordierite-gedrite gneiss of Thor-Odin dome, Monashee complex, Canadian Cordillera. *Chem. Geol.* **240**, 85-102.

HOFFER, E. & GRANT, J.A. (1980): Experimental investigation of the formation of cordierite–orthopyroxene paragneisses in pelitic rocks. *Contrib. Mineral. Petrol.* **73**, 15-22.

HÖY, T. (1989): The age, chemistry, and tectonic setting of the Middle Proterozoic Moyie sills, Purcell Supergroup, southeastern British Columbia. *Can. J. Earth Sci.* **29**, 2305-2317.

IRVING, A.J. & ASHLEY, P.M. (1976): Amphibole–olivine–spinel, cordierite–anthophyllite and related hornfelses associated with metamorphosed serpentinites in the Goobarragandra District, near Tumut, New South Wales. *J. Geol. Soc. Aust.* **23**, 19-43.

JAMES, R.S., GRIEVE, R.A.F. & PAUK, L. (1978): The petrology of cordierite–anthophyllite gneisses and associated mafic and pelitic gneisses at Manitouwadge, Ontario. *Am. J. Sci.* **278,** 41-63.

JENNER, G.A. (1996): Trace-element geochemistry of igneous rocks; geochemical nomenclature and analytical geochemistry. *In* Trace-Element Geochemistry of Volcanic Rocks; Applications for Massive Sulphide Exploration (D.A. Wyman, ed.). *Geol. Assoc. Can., Short-Course Notes* **12**, 51-77.

JOHNSON, B.J. (2006): Extensional shear zone, granitic melts, and linkage of overstepping normal faults bounding the Shuswap metamorphic core complex, British Columbia. *Geol. Soc. Am., Bull.* **118**, 366-382.

KRETZ, R. (1983): Symbols for rock-forming minerals. *Am. Mineral.* **68**, 77-279.

KRUSE, S., MCNEILL, P. & WILLIAMS, P.F. (2004): A geological map of the Thor–Odin dome, Monashee complex, B.C. http://www.unb.ca/fredericton/science/geology/monashee

KUIPER, Y. (2003): *Isotopic Constraints on Timing of Deformation and Metamorphism in the Thor–odin Dome, Monashee Complex, Southeastern British Columbia*. Ph.D. thesis, Univ. of New Brunswick, Fredricton, New Brunswick.

LE MAITRE, R.W. (1976): Some problems of the projection of chemical data into mineralogical classifications. *Contrib. Mineral. Petrol.* **56**, 181-189.

MCNEILL, P.D. & WILLIAMS, P.F. (2003): Structural evolution of migmatites of the Thor–Odin area of the Monashee complex, southern British Columbia. Cordilleran Tectonics Workshop 2003, Carleton University, Ottawa, Ontario.

MCNICOLL, V.J. & BROWN, R.L. (1995): The Monashee décollement at Cariboo Alp, southern flank of the Monashee complex, southern British Columbia, Canada. *J. Struct. Geol.* **17**, 17-30.

MONGER, J.W.H., PRICE, R.A. & TEMPELMAN-KLUIT, D.J. (1982): Tectonic accretion and the origin of the two major metamorphic and plutonic welts in the Canadian Cordillera. *Geology* **10**, 70-75.

MOORE, J.M. & WATERS, D.J. (1990): Geochemistry and origin of cordierite–orthoamphibole/orthopyroxene–phlogopite rocks from Namaqualand, South Africa. *Chem. Geol.* **85**, 77-100.

NORLANDER, B.H., WHITNEY, D.L., TEYSSIER, C. & VANDERHAEGHE, O. (2002): Partial melting and decompression of the Thor–Odin Dome, Shuswap metamorphic core complex, Canadian Cordillera. *Lithos* **61**, 103-125.

PARKINSON, D.L. (1991): Age and isotopic character of Early Proterozoic basement gneisses in the southern Monashee Complex, southeastern British Columbia. *Can. J. Earth Sci.* **28**, 1159-1168.

PARKINSON, D.L. (1992): *Age and Tectonic Evolution of the Southern Monashee Complex, Southeastern British Columbia; a Window into the Deep Crust*. Ph.D. thesis, Univ. of California, Santa Barbara, California.

PARRISH, R.R. (1995): Thermal evolution of the southeastern Canadian Cordillera, *Can. J. Earth Sci.* **32**, 1618-1642.

PARRISH, R.R., CARR, S.D. & PARKINSON, D.L. (1988): Eocene extensional tectonics and geochronology of the southern Omineca Belt, British Columbia and Washington. *Tectonics* **7**, 181-212.

PECK, W.H. & SMITH, M.S. (2005): Cordierite–gedrite rocks from the Central Metasedimentary Belt boundary thrust zone (Grenville Province, Ontario): Mesoproterozoic metavolcanic rocks with affinities to the Composite Arc Belt. *Can. J. Earth Sci.* **42**, 1815-1828.

REESOR, J.E. & MOORE, J.M. (1971): Petrology and structure of Thor–Odin gneiss dome, Shuswap metamorphic complex, British Columbia. *Geol. Surv. Can., Pap.* **195**.

ROBINSON, P. & JAFFE, H.W. (1969a): Chemographic exploration of amphibole assemblages from central Massachusetts and southwestern New Hampshire. *Mineral. Soc. Am., Spec. Pap.* **2**, 251-274.

ROBINSON, P. & JAFFE, H.W. (1969b): Aluminous enclaves in gedrite–cordierite gneiss from southwestern New Hampshire. *Am. J. Sci.* **267**, 389-421.

ROLLINSON, H.R. (1993): *Using Geochemical Data: Evaluation, Presentation, Interpretation*. Longman Scientific and Technical, John Wiley and Sons,New York, N.Y.

ROSS, G.M. (1991): Tectonic setting of the Windermere Supergroup revisited. *Geology* **19**, 1125- 1128.

ROSS, G.M., VILLENEUVE, M.E., PARRISH, R.R. & THÉRIAULT, R.J. (1993): Tectonic assembly of crystalline basement, Alberta Basin; implications for mantle evolution and ancestry of Canada's Pacific margin. *Lithoprobe Rep.* **31**, 134-143.

SAUNDERS, A.D., TARNEY, J., MARSH, N.G. & WOOD, D.A. (1980): Ophiolites as ocean crust or marginal basin crust: a geochemical approach (A. Panayiotou, ed.). *In* Ophiolites: Proc. Int. Ophiolite Symp. (Nicosia). Ministry of Agriculture and Natural Resources, Geological Survey Department, Cyprus (171-180).

SCHUMACHER, J.C. (1988): Stratigraphy and geochemistry of the Ammonoosuc Volcanics, central Massachusetts and southwestern New Hampshire. *Am. J. Sci.* **288**, 619-663.

SEVIGNY, J.H. (1988): Geochemistry of Late Proterozoic amphibolites and ultramafic rocks, southeastern Canadian Cordillera. *Can. J. Earth Sci.* **25**, 1323-1337.

SEVIGNY, J.H. & THÉRIAULT, R.J. (2003): Geochemistry and Sr–Nd isotopic composition of Eocene lamprophyre dykes, southeastern British Columbia. *Can. J. Earth Sci.* **40**, 853-864.

SIMONY, P.S., GHENT, E.D., CRAW, D., MITCHELL, W. & ROBBINS, D.G. (1980): Structural and metamorphic evolution of the northeast flank of the Shuswap Complex, southern Canoe complexes. *In* Cordilleran Metamorphic Core Complexes (M.D. Crittenden Jr., P.J. Coney & G.H. Davis, eds.). *Geol. Soc. Am., Mem.* **153**, 445-461.

SMITH, M.S., DYMEK, R.F. & SCHNEIDERMAN, J.S. (1992): Implications of trace-element geochemistry for the origin of cordierite–orthoamphibole rocks from Orijarvi, SW Finland. *J. Geol.* **100**, 545-559.

SPEAR, F.S. (1993): *Metamorphic Phase Equilibria and Pressure – Temperature – Time Paths*. Mineralogical Society of America, Washington, D.C.

SPEAR, F.S. & SCHUMACHER, J.C. (1982): Origin of cordierite–anthophyllite rocks. *In* Amphiboles; Petrology and Experimental Phase Relations (D.R. Veblen & P.H. Ribbe, eds.). *Reviews in Mineralogy* **9B**, 160-163.

SUN, S.-S. & MCDONOUGH, W.F. (1989): Chemical and isotopic systematics of oceanic basalts: implications for mantle composition and processes. *In* Magmatism in Ocean Basins (A.D. Saunders & M.J. Norry, eds.). *Geol. Soc., Spec. Publ.* **42**, 313-345.

TAYLOR, S.R. & MCLENNAN, S.M. (1985): *The Continental Crust: Its Composition and Evolution*. Blackwell Scientific, Oxford, U.K.

TAYLOR, S.R. & MCLENNAN, S.M. (1995): The geochemical evolution of the continental crust. *Rev. Geophys.* **33**, 241-265.

TEYSSIER, C., FERRÉ, E., WHITNEY, D.L., NORLANDER, B., VANDERHAEGHE, O. & PARKINSON, D. (2005): Flow of partially molten crust and origin of detachments during collapse of the Cordilleran orogen. *In* High-Strain Zones: Structures and Physical Properties (D. Bruhn & L. Burlini, eds.). *Geol. Soc., Spec. Publ.* **245**, 39-64.

VALLANCE, T.G. (1967): Mafic rock alteration and isochemical development of some cordierite–anthophyllite rocks. *J. Petrol.* **8**, 84-96.

VANDERHAEGHE, O., TEYSSIER, C., MCDOUGALL, I. & DUNLAP, D.W. (2003): Cooling and exhumation of the Shuswap metamorphic core complex constrained by $^{40}Ar/^{39}Ar$ thermochronology, *Geol. Soc. Am. Bull.* **115**, 200-216.

VANDERHAEGHE, O., TEYSSIER, C. & WYSOCZANSKI, R. (1999): Structural and geochronological constraints on the role of partial melting during the formation of the Shuswap metamorphic core complex at the latitude of the Thor–Odin dome, British Columbia. *Can. J. Earth Sci.* **36**, 917-943.

WANLESS, R.K. & REESOR, J.E. (1975): Precambrian zircon age of orthogneiss in the Shuswap Metamorphic Complex, British Columbia. *Can. J. Earth Sci.* **12**, 326-332.

WHEELER, J.O. & MCFEELY, P. (1991): Tectonic assemblage map of the Canadian Cordillera and adjacent parts of the United States of America. *Geol. Surv. Can., Map* **17121** (scale 1:2 000 000).

WILLIAMS, P.F. & JIANG, D. (2005): An investigation of lower crustal deformation: evidence for channel flow and its implications for tectonics and structural studies. *Struct. Geol.* **27**, 1486-1504.

WINCHESTER, J.A. & FLOYD, P.A. (1977): Geochemical discrimination of different magma series and their differentiation products using immobile elements. *Chem. Geol.* **20**, 325-343.

YOUNG, G.M. (1973): Tillites and aluminous quartzites as possible time markers for middle Precambrian (Aphebian) rocks of North America. *Geol. Assoc. Can., Spec. Pap.* **12**, 97-127.

*Received September 20, 2005, revised manuscript accepted September 19, 2006.*

# APPENDIX A. ANALYTICAL METHODS

*Whole-rock major and trace-element geochemistry*

Selected samples were analyzed for major elements and some trace elements (Cr, Ni, Cu, Zn, Ga, Y, Zr, Nb, Ba) by X-ray fluorescence (XRF) on fused disks using a Philips PW 2400 X-ray fluorescence spectrometer at the University of Ottawa. XRF precision is based on six replicate runs and was 0.71% for $SiO_2$, 0.27% for $Al_2O_3$, 0.74% for $K_2O$, 6.4% for Zn. The accuracy was monitored using international references DR–N and SY–2 and was within 0.6% for $SiO_2$, 0.3% for $Al_2O_3$, 0.8% for $K_2O$, 1.6% for Zn, and better than 1% and 10% for other major and trace elements, respectively. Levels of the REE and other trace elements in selected samples were established at Geoscience Laboratories in Sudbury, Ontario and at ACME analytical laboratories in Vancouver, British Columbia, by inductively coupled plasma – mass spectrometry (ICP–MS) using a HP 4500plus quadrupole instrument following a $HNO_3$–$HClO_4$–HF–HCl digestion. This acid-digestion technique was selected because of lower detection-limits for many elements and the large number of elements that could be included. The precision of the REE analyses is based on seven replicates and was mostly better than 10%, but samples with concentrations close to detection limits had precision of only 20%. The accuracy of REE analyses was monitored by international references SY–4, BIR–1 and GSR–2; it was better than 10% for materials with high concentrations of REE. As some trace-element-rich accessory phases are resistant to acid digestion, several samples were analyzed in duplicates using more rigorous combination of fusion and acid digestion. A comparison of six samples had precision for the REE mostly better than 10%, and therefore concerns about the effects of incomplete digestion by acid are minimal.

*Whole-rock isotope geochemistry*

Rubidium–strontium and samarium–neodymium isotopic analyses were carried out at Carleton University. Powdered samples were each dissolved with 1 mL of doubly distilled $HNO_3$ and HF for two to seven days. The samples were loaded onto columns with Dowex 50WX8 resin for Sr and initial REE-group separation. The Sm–Nd isotopic concentration and isotope-dilution fractions were pipetted into Teflon columns using 2× 0.15N HCl to separate these elements from the rest of the REE. The Nd was removed using 2× 0.17N HCl.

The Sr and Sm–Nd fractions were loaded separately on outgassed single Ta filaments and double Re filaments for analysis on a Finnegan MAT 261 thermal ionization mass spectrometer. The isotopic composition fractions were measured using the Faraday multicollector routine, which collects 15 blocks of 10 scans, with on-line corrections for drift and mass fractionation and statistical analysis. The errors in $^{87}Sr/^{86}Sr$ and $^{143}Nd/^{144}Nd$ are reported to 2σ (95%) confidence intervals and were directly measured. The ratios $^{87}Rb/^{86}Sr$ and $^{147}Sm/^{144}Nd$ were calculated based on the measured Rb and Sr concentrations from the whole-rock ICP–MS values. The estimated uncertainties, at the 2σ level, equate to a precision of 1% for the ratios $^{147}Sm/^{144}Nd$ and $^{87}Sr/^{86}Sr$, and the concentrations are reproducible to 0.5%. On the basis of numerous runs from September 1992 to October 2004, the La Jolla standard gave an average $^{143}Nd/^{144}Nd$ value of 0.511876 ± 0.00018, and the Sr standard NBS–987 gave an average $^{87}Sr/^{86}Sr$ value of 0.71025 ± 0.00003.